48. Janssen HL, Reesink HW, Lawitz EJ, Zeuzem S, Rodriguez-Torres M, Patel K, et al. Treatment of HCV infection by targeting microRNA. N Engl J Med. 2013;368:1685–94.
49. Jopling CL, Yi M, Lancaster AM, Lemon SM, Sarnow P. Modulation of hepatitis C virus RNA abundance by a liver-specific MicroRNA. Science. 2005;309:1577–81.
50. Fukuhara T, Matsuura Y. Role of miR-122 and lipid metabolism in HCV infection. J Gastroenterol. 2013;48:169–76.
51. Bouchie A. First microRNA mimic enters clinic. Nat Biotechnol. 2013;31:577.
52. Yang F, Yin Y, Wang F, Wang Y, Zhang L, Tang Y, et al. miR-17-5p Promotes migration of human hepatocellular carcinoma cells through the p38 mitogen-activated protein kinase-heat shock protein 27 pathway. Hepatology. 2010;51:1614–23.
53. Liu WH, Yeh SH, Lu CC, Yu SL, Chen HY, Lin CY, et al. MicroRNA-18a prevents estrogen receptor-alpha expression, promoting proliferation of hepatocellular carcinoma cells. Gastroenterology. 2009;136:683–93.
54. Wang B, Majumder S, Nuovo G, Kutay H, Volinia S, Patel T, et al. Role of microRNA-155 at early stages of hepatocarcinogenesis induced by choline-deficient and amino acid-defined diet in C57BL/6 mice. Hepatology. 2009;50:1152–61.
55. Jiang R, Deng L, Zhao L, Li X, Zhang F, Xia Y, et al. miR-22 promotes HBV-related hepatocellular carcinoma development in males. Clin Cancer Res. 2011;17:5593–603.
56. Wang B, Hsu SH, Frankel W, Ghoshal K, Jacob ST. Stat3-mediated activation of microRNA-23a suppresses gluconeogenesis in hepatocellular carcinoma by down-regulating glucose-6-phosphatase and peroxisome proliferator-activated receptor gamma, coactivator 1 alpha. Hepatology. 2012;56:186–97.
57. Fu X, Meng Z, Liang W, Tian Y, Wang X, Han W, et al. miR-26a enhances miRNA biogenesis by targeting Lin28B and Zcchc11 to suppress tumor growth and metastasis. Oncogene. 2013 (in press).
58. Ji J, Shi J, Budhu A, Yu Z, Forgues M, Roessler S, et al. MicroRNA expression, survival, and response to interferon in liver cancer. N Engl J Med. 2009;361:1437–47.
59. Yao J, Liang L, Huang S, Ding J, Tan N, Zhao Y, et al. MicroRNA-30d promotes tumor invasion and metastasis by targeting Galphai2 in hepatocellular carcinoma. Hepatology. 2010;51:846–56.
60. Varnholt H, Drebber U, Schulze F, Wedemeyer I, Schirmacher P, Dienes HP, et al. MicroRNA gene expression profile of hepatitis C virus-associated hepatocellular carcinoma. Hepatology. 2008;47:1223–32.
61. Shen G, Jia H, Tai Q, Li Y, Chen D. miR-106b downregulates adenomatous polyposis coli and promotes cell proliferation in human hepatocellular carcinoma. Carcinogenesis. 2013;34:211–9.
62. Ma S, Tang KH, Chan YP, Lee TK, Kwan PS, Castilho A, et al. miR-130b Promotes CD133(+) liver tumor-initiating cell growth and self-renewal via tumor protein 53-induced nuclear protein 1. Cell Stem Cell. 2010;7:694–707.
63. Liu S, Guo W, Shi J, Li N, Yu X, Xue J, et al. MicroRNA-135a contributes to the development of portal vein tumor thrombus by promoting metastasis in hepatocellular carcinoma. J Hepatol. 2012;56:389–96.
64. Zhang X, Liu S, Hu T, He Y, Sun S. Up-regulated microRNA-143 transcribed by nuclear factor kappa B enhances hepatocarcinoma metastasis by repressing fibronectin expression. Hepatology. 2009;50:490–9.
65. Zhu K, Pan Q, Zhang X, Kong LQ, Fan J, Dai Z, et al. MiR-146a enhances angiogenic activity of endothelial cells in hepatocellular carcinoma by promoting PDGFRA expression. Carcinogenesis. 2013;34:2071–9.
66. Luedde T. MicroRNA-151 and its hosting gene FAK (focal adhesion kinase) regulate tumor cell migration and spreading of hepatocellular carcinoma. Hepatology. 2010;52:1164–6.
67. Ding J, Huang S, Wu S, Zhao Y, Liang L, Yan M, et al. Gain of miR-151 on chromosome 8q24.3 facilitates tumour cell migration and spreading through downregulating RhoGDIA. Nat Cell Biol. 2010;12:390–9.
68. Yan XL, Jia YL, Chen L, Zeng Q, Zhou JN, Fu CJ, et al. Hepatocellular carcinoma-associated mesenchymal stem cells promote hepatocarcinoma progression: role of the S100A4-miR155-SOCS1-MMP9 axis. Hepatology. 2013;57:2274–86.
69. Zhang S, Shan C, Kong G, Du Y, Ye L, Zhang X. MicroRNA-520e suppresses growth of hepatoma cells by targeting the NF-κB-inducing kinase (NIK). Oncogene. 2012;31:3607–20.
70. Wang B, Hsu SH, Majumder S, Kutay H, Huang W, Jacob ST, et al. TGFbeta-mediated upregulation of hepatic miR-181b promotes hepatocarcinogenesis by targeting TIMP3. Oncogene. 2010;29:1787–97.
71. Ji J, Yamashita T, Budhu A, Forgues M, Jia HL, Li C, et al. Identification of microRNA-181 by genome-wide screening as a critical player in EpCAM-positive hepatic cancer stem cells. Hepatology. 2009;50:472–80.
72. Goeppert B, Schmezer P, Dutruel C, Oakes C, Renner M, Breinig M, et al. Down-regulation of tumor suppressor A kinase anchor protein 12 in human hepatocarcinogenesis by epigenetic mechanisms. Hepatology. 2010;52:2023–33.
73. Petrelli A, Perra A, Cora D, Sulas P, Menegon S, Manca C, et al. MiRNA/gene profiling unveils early molecular changes and NRF2 activation in a rat model recapitulating human HCC. Hepatology. 2013 (in press).
74. Ying Q, Liang L, Guo W, Zha R, Tian Q, Huang S, et al. Hypoxia-inducible microRNA-210 augments the metastatic potential of tumor cells by targeting vacuole membrane protein 1 in hepatocellular carcinoma. Hepatology. 2011;54:2064–75.
75. Chen PJ, Yeh SH, Liu WH, Lin CC, Huang HC, Chen CL, et al. Androgen pathway stimulates microRNA-216a transcription to suppress the tumor suppressor in lung cancer-1 gene in early hepatocarcinogenesis. Hepatology. 2012;56:632–43.
76. Xia H, Ooi LL, Hui KM. MicroRNA-216a/217-induced epithelial–mesenchymal transition targets PTEN and SMAD7 to promote drug resistance and recurrence of liver cancer. Hepatology. 2013;58:629–41.
77. Callegari E, Elamin BK, Giannone F, Milazzo M, Altavilla G, Fornari F, et al. Liver tumorigenicity promoted by microRNA-221 in a mouse transgenic model. Hepatology. 2012;56:1025–33.
78. Yuan Q, Loya K, Rani B, Möbus S, Balakrishnan A, Lamle J, et al. MicroRNA-221 overexpression accelerates hepatocyte proliferation during liver regeneration. Hepatology. 2013;57:299–310.
79. Gramantieri L, Fornari F, Ferracin M, Veronese A, Sabbioni S, Calin GA, et al. MicroRNA-221 targets Bmf in hepatocellular carcinoma and correlates with tumor multifocality. Clin Cancer Res. 2009;15:5073–81.
80. Fornari F, Gramantieri L, Ferracin M, Veronese A, Sabbioni S, Calin GA, et al. MiR-221 controls CDKN1C/p57 and CDKN1B/p27 expression in human hepatocellular carcinoma. Oncogene. 2008;27:5651–61.
81. Pineau P, Volinia S, McJunkin K, Marchio A, Battiston C, Terris B, et al. miR-221 overexpression contributes to liver tumorigenesis. Proc Natl Acad Sci USA. 2010;107:264–9.
82. Ladeiro Y, Couchy G, Balabaud C, Bioulac-Sage P, Pelletier L, Rebouissou S, et al. MicroRNA profiling in hepatocellular tumors is associated with clinical features and oncogene/tumor suppressor gene mutations. Hepatology. 2008;47:1955–63.
83. Lan SH, Wu SY, Zuchini R, Lin XZ, Su IJ, Tsai TF, et al. Autophagy suppresses tumorigenesis of hepatitis B virus-

associated hepatocellular carcinoma through degradation of miR-224. Hepatology. 2013 (in press).
84. Scisciani C, Vossio S, Guerrieri F, Schinzari V, De Iaco R, D'Onorio de Meo P, et al. Transcriptional regulation of miR-224 upregulated in human HCCs by NFκB inflammatory pathways. J Hepatol. 2012;56:855–61.
85. Gao P, Wong CC, Tung EK, Lee JM, Wong CM, Ng IO. Deregulation of microRNA expression occurs early and accumulates in early stages of HBV-associated multistep hepatocarcinogenesis. J Hepatol. 2011;54:1177–84.
86. Wang Y, Lee AT, Ma JZ, Wang J, Ren J, Yang Y, et al. Profiling microRNA expression in hepatocellular carcinoma reveals microRNA-224 up-regulation and apoptosis inhibitor-5 as a microRNA-224-specific target. J Biol Chem. 2008;283:13205–15.
87. Lin J, Huang S, Wu S, Ding J, Zhao Y, Liang L, et al. MicroRNA-423 promotes cell growth and regulates G(1)/S transition by targeting p21Cip1/Waf1 in hepatocellular carcinoma. Carcinogenesis. 2011;32:1641–7.
88. Yang H, Cho ME, Li TW, Peng H, Ko KS, Mato JM, et al. MicroRNAs regulate methionine adenosyltransferase 1A expression in hepatocellular carcinoma. J Clin Invest. 2013;123:285–98.
89. Zhang LY, Liu M, Li X, Tang H. miR-490-3p modulates cell growth and epithelial to mesenchymal transition of hepatocellular carcinoma cells by targeting endoplasmic reticulum-Golgi intermediate compartment protein 3 (ERGIC3). J Biol Chem. 2013;288:4035–47.
90. Lim L, Balakrishnan A, Huskey N, Jones KD, Jodari M, Ng R, et al. MiR-494 within an oncogenic MicroRNA megacluster regulates G1/S transition in liver tumorigenesis through suppression of MCC. Hepatology. 2013 (in press).
91. Toffanin S, Hoshida Y, Lachenmayer A, Villanueva A, Cabellos L, Minguez B, et al. MicroRNA-based classification of hepatocellular carcinoma and oncogenic role of miR-517a. Gastroenterology. 2011;140(1618–1628):e1616.
92. Zhang L, Yang L, Liu X, Chen W, Chang L, Chen L, et al. MicroRNA-657 promotes tumorigenesis in hepatocellular carcinoma by targeting transducin-like enhancer protein 1 through nuclear factor kappa B pathways. Hepatology. 2013;57:1919–30.
93. Law PT, Qin H, Ching AK, Lai KP, Co NN, He M, et al. Deep sequencing of small RNA transcriptome reveals novel non-coding RNAs in hepatocellular carcinoma. J Hepatol. 2013;58:1165–73.
94. Wang Y, Lu Y, Toh ST, Sung WK, Tan P, Chow P, et al. Lethal-7 is down-regulated by the hepatitis B virus x protein and targets signal transducer and activator of transcription 3. J Hepatol. 2010;53:57–66.
95. Au SL, Wong CC, Lee JM, Fan DN, Tsang FH, Ng IO, et al. Enhancer of zeste homolog 2 epigenetically silences multiple tumor suppressor microRNAs to promote liver cancer metastasis. Hepatology. 2012;56:622–31.
96. Ji J, Zhao L, Budhu A, Forgues M, Jia HL, Qin LX, et al. Let-7g targets collagen type I alpha2 and inhibits cell migration in hepatocellular carcinoma. J Hepatol. 2010;52:690–7.
97. Fang Y, Xue JL, Shen Q, Chen J, Tian L. MicroRNA-7 inhibits tumor growth and metastasis by targeting the phosphoinositide 3-kinase/Akt pathway in hepatocellular carcinoma. Hepatology. 2012;55:1852–62.
98. Yan Y, Luo YC, Wan HY, Wang J, Zhang PP, Liu M, et al. MicroRNA-10a is involved in the metastatic process by regulating Eph tyrosine kinase receptor A4-mediated epithelial–mesenchymal transition and adhesion in hepatoma cells. Hepatology. 2013;57:667–77.
99. Maurel M, Jalvy S, Ladeiro Y, Combe C, Vachet L, Sagliocco F, et al. A functional screening identifies five microRNAs controlling glypican-3: role of miR-1271 down-regulation in hepatocellular carcinoma. Hepatology. 2013;57:195–204.
100. Wang Y, Jiang L, Ji X, Yang B, Zhang Y, Fu XD. Hepatitis B viral RNA directly mediates down-regulation of the tumor suppressor microRNA miR-15a/miR-16-1 in hepatocytes. J Biol Chem. 2013;288:18484–93.
101. Yang X, Liang L, Zhang XF, Jia HL, Qin Y, Zhu XC, et al. MicroRNA-26a suppresses tumor growth and metastasis of human hepatocellular carcinoma by targeting interleukin-6-Stat3 pathway. Hepatology. 2013;58:158–70.
102. Kota J, Chivukula RR, O'Donnell KA, Wentzel EA, Montgomery CL, Hwang HW, et al. Therapeutic microRNA delivery suppresses tumorigenesis in a murine liver cancer model. Cell. 2009;137:1005–17.
103. Xiong Y, Fang JH, Yun JP, Yang J, Zhang Y, Jia WH, et al. Effects of microRNA-29 on apoptosis, tumorigenicity, and prognosis of hepatocellular carcinoma. Hepatology. 2010;51:836–45.
104. Fang JH, Zhou HC, Zeng C, Yang J, Liu Y, Huang X, et al. MicroRNA-29b suppresses tumor angiogenesis, invasion, and metastasis by regulating matrix metalloproteinase 2 expression. Hepatology. 2011;54:1729–40.
105. Bae HJ, Noh JH, Kim JK, Eun JW, Jung KH, Kim MG, et al. MicroRNA-29c functions as a tumor suppressor by direct targeting oncogenic SIRT1 in hepatocellular carcinoma. Oncogene. 2013 (in press).
106. Yang P, Li QJ, Feng Y, Zhang Y, Markowitz GJ, Ning S, et al. TGF-β-miR-34a-CCL22 signaling-induced Treg cell recruitment promotes venous metastases of HBV-positive hepatocellular carcinoma. Cancer Cell. 2012;22:291–303.
107. Petrelli A, Perra A, Schernhuber K, Cargnelutti M, Salvi A, Migliore C, et al. Sequential analysis of multistage hepatocarcinogenesis reveals that miR-100 and PLK1 dysregulation is an early event maintained along tumor progression. Oncogene. 2012;31:4517–26.
108. Li D, Liu X, Lin L, Hou J, Li N, Wang C, et al. MicroRNA-99a inhibits hepatocellular carcinoma growth and correlates with prognosis of patients with hepatocellular carcinoma. J Biol Chem. 2011;286:36677–85.
109. Wang L, Zhang X, Jia LT, Hu SJ, Zhao J, Yang JD, et al. c-Myc-mediated epigenetic silencing of microRNA-101 contributes to dysregulation of multiple pathways in hepatocellular carcinoma. Hepatology. 2013 (in press).
110. Su H, Yang JR, Xu T, Huang J, Xu L, Yuan Y, et al. MicroRNA-101, down-regulated in hepatocellular carcinoma, promotes apoptosis and suppresses tumorigenicity. Cancer Res. 2009;69:1135–42.
111. Li S, Fu H, Wang Y, Tie Y, Xing R, Zhu J, et al. MicroRNA-101 regulates expression of the v-fos FBJ murine osteosarcoma viral oncogene homolog (FOS) oncogene in human hepatocellular carcinoma. Hepatology. 2009;49:1194–202.
112. Wang B, Hsu SH, Wang X, Kutay H, Bid HK, Yu J, et al. Reciprocal regulation of miR-122 and c-Myc in hepatocellular cancer: role of E2F1 and TFDP2. Hepatology. 2013 (in press).
113. Song K, Han C, Zhang J, Lu D, Dash S, Feitelson M, et al. Epigenetic regulation of MicroRNA-122 by peroxisome proliferator activated receptor-gamma and hepatitis b virus X protein in hepatocellular carcinoma cells. Hepatology. 2013 (in press).
114. Zeng C, Wang R, Li D, Lin XJ, Wei QK, Yuan Y, et al. A novel GSK-3 beta-C/EBP alpha-miR-122-insulin-like growth factor 1 receptor regulatory circuitry in human hepatocellular carcinoma. Hepatology. 2010;52:1702–12.
115. Gramantieri L, Ferracin M, Fornari F, Veronese A, Sabbioni S, Liu CG, et al. Cyclin G1 is a target of miR-122a, a microRNA frequently down-regulated in human hepatocellular carcinoma. Cancer Res. 2007;67:6092–9.

116. Zheng F, Liao YJ, Cai MY, Liu YH, Liu TH, Chen SP, et al. The putative tumour suppressor microRNA-124 modulates hepatocellular carcinoma cell aggressiveness by repressing ROCK2 and EZH2. Gut. 2012;61:278–89.
117. Furuta M, Kozaki KI, Tanaka S, Arii S, Imoto I, Inazawa J. miR-124 and miR-203 are epigenetically silenced tumor-suppressive microRNAs in hepatocellular carcinoma. Carcinogenesis. 2010;31:766–76.
118. Kim JK, Noh JH, Jung KH, Eun JW, Bae HJ, Kim MG, et al. Sirtuin7 oncogenic potential in human hepatocellular carcinoma and its regulation by the tumor suppressors MiR-125a-5p and MiR-125b. Hepatology. 2013;57:1055–67.
119. Fan DN, Tsang FH, Tam AH, Au SL, Wong CC, Wei L, et al. Histone lysine methyltransferase, suppressor of variegation 3–9 homolog 1, promotes hepatocellular carcinoma progression and is negatively regulated by microRNA-125b. Hepatology. 2013;57:637–47.
120. Gong J, Zhang JP, Li B, Zeng C, You K, Chen MX, et al. MicroRNA-125b promotes apoptosis by regulating the expression of Mcl-1, Bcl-w and IL-6R. Oncogene. 2013;32:3071–9.
121. Alpini G, Glaser SS, Zhang JP, Francis H, Han Y, Gong J, et al. Regulation of placenta growth factor by microRNA-125b in hepatocellular cancer. J Hepatol. 2011;55:1339–45.
122. Liang L, Wong CM, Ying Q, Fan DN, Huang S, Ding J, et al. MicroRNA-125b suppressesed human liver cancer cell proliferation and metastasis by directly targeting oncogene LIN28B2. Hepatology. 2010;52:1731–40.
123. Wong CC, Wong CM, Tung EK, Au SL, Lee JM, Poon RT, et al. The microRNA miR-139 suppresses metastasis and progression of hepatocellular carcinoma by down-regulating Rho-kinase 2. Gastroenterology. 2011;140:322–31.
124. Yang H, Fang F, Chang R, Yang L. MicroRNA-140-5p suppresses tumor growth and metastasis by targeting transforming growth factor β receptor 1 and fibroblast growth factor 9 in hepatocellular carcinoma. Hepatology. 2013;58:205–17.
125. Takata A, Otsuka M, Yoshikawa T, Kishikawa T, Hikiba Y, Obi S, et al. MicroRNA-140 acts as a liver tumor suppressor by controlling NF-κB activity by directly targeting DNA methyltransferase 1 (Dnmt1) expression. Hepatology. 2013;57:162–70.
126. Banaudha K, Kaliszewski M, Korolnek T, Florea L, Yeung ML, Jeang KT, et al. MicroRNA silencing of tumor suppressor DLC-1 promotes efficient hepatitis C virus replication in primary human hepatocytes. Hepatology. 2011;53:53–61.
127. Law PT, Ching AK, Chan AW, Wong QW, Wong CK, To KF, et al. MiR-145 modulates multiple components of the insulin-like growth factor pathway in hepatocellular carcinoma. Carcinogenesis. 2012;33:1134–41.
128. Gailhouste L, Gomez-Santos L, Hagiwara K, Hatada I, Kitagawa N, Kawaharada K, et al. miR-148a plays a pivotal role in the liver by promoting the hepatospecific phenotype and suppressing the invasiveness of transformed cells. Hepatology. 2013;58:1153–65.
129. Xu X, Fan Z, Kang L, Han J, Jiang C, Zheng X, et al. Hepatitis B virus X protein represses miRNA-148a to enhance tumorigenesis. J Clin Invest. 2013;123:630–45.
130. Zhang JP, Zeng C, Xu L, Gong J, Fang JH, Zhuang SM. MicroRNA-148a suppresses the epithelial–mesenchymal transition and metastasis of hepatoma cells by targeting Met/Snail signaling. Oncogene. 2013 (in press).
131. Han H, Sun D, Li W, Shen H, Zhu Y, Li C, et al. A c-Myc-MicroRNA functional feedback loop affects hepatocarcinogenesis. Hepatology. 2013;57:2378–89.
132. Huang J, Wang Y, Guo Y, Sun S. Down-regulated microRNA-152 induces aberrant DNA methylation in hepatitis B virus-related hepatocellular carcinoma by targeting DNA methyltransferase 1. Hepatology. 2010;52:60–70.
133. Ding J, Huang S, Wang Y, Tian Q, Zha R, Shi H, et al. Genome-wide screening reveals that miR-195 targets the TNF-α/NF-κB pathway by down-regulating IκB kinase alpha and TAB 3 in hepatocellular carcinoma. Hepatology. 2013;58:654–66.
134. Wang R, Zhao N, Li S, Fang JH, Chen MX, Yang J, et al. MicroRNA-195 suppresses angiogenesis and metastasis of hepatocellular carcinoma by inhibiting the expression of VEGF, VAV2, and CDC42. Hepatology. 2013;58:642–53.
135. Xu T, Zhu Y, Xiong Y, Ge YY, Yun JP, Zhuang SM. MicroRNA-195 suppresses tumorigenicity and regulates G1/S transition of human hepatocellular carcinoma cells. Hepatology. 2009;50:113–21.
136. Yuan JH, Yang F, Chen BF, Lu Z, Huo XS, Zhou WP, et al. The histone deacetylase 4/SP1/microrna-200a regulatory network contributes to aberrant histone acetylation in hepatocellular carcinoma. Hepatology. 2011;54:2025–35.
137. Shih TC, Tien YJ, Wen CJ, Yeh TS, Yu MC, Huang CH, et al. MicroRNA-214 downregulation contributes to tumor angiogenesis by inducing secretion of the hepatoma-derived growth factor in human hepatoma. J Hepatol. 2012;57:584–91.
138. Wong QW, Lung RW, Law PT, Lai PB, Chan KY, To KF, et al. MicroRNA-223 is commonly repressed in hepatocellular carcinoma and potentiates expression of Stathmin1. Gastroenterology. 2008;135:257–69.
139. Guichard C, Amaddeo G, Imbeaud S, Ladeiro Y, Pelletier L, Maad IB, et al. Integrated analysis of somatic mutations and focal copy-number changes identifies key genes and pathways in hepatocellular carcinoma. Nat Genet. 2012;44:694–8.
140. Chang Y, Yan W, He X, Zhang L, Li C, Huang H, et al. miR-375 inhibits autophagy and reduces viability of hepatocellular carcinoma cells under hypoxic conditions. Gastroenterology. 2012;143(177–187):e178.
141. He XX, Chang Y, Meng FY, Wang MY, Xie QH, Tang F, et al. MicroRNA-375 targets AEG-1 in hepatocellular carcinoma and suppresses liver cancer cell growth in vitro and in vivo. Oncogene. 2012;31:3357–69.
142. You X, Liu F, Zhang T, Li Y, Ye L, Zhang X. Hepatitis B virus X protein upregulates oncogene Rab18 to result in the dysregulation of lipogenesis and proliferation of hepatoma cells. Carcinogenesis. 2013;34:1644–52.
143. Buurman R, Gürlevik E, Schäffer V, Eilers M, Sandbothe M, Kreipe H, et al. Histone deacetylases activate hepatocyte growth factor signaling by repressing microRNA-449 in hepatocellular carcinoma cells. Gastroenterology. 2012;143:811–20. e811–15.
144. Tao ZH, Wan JL, Zeng LY, Xie L, Sun HC, Qin LX, et al. miR-612 suppresses the invasive-metastatic cascade in hepatocellular carcinoma. J Exp Med. 2013;210:789–803.
145. Zhang JF, He ML, Fu WM, Wang H, Chen LZ, Zhu X, et al. Primate-specific microRNA-637 inhibits tumorigenesis in hepatocellular carcinoma by disrupting signal transducer and activator of transcription 3 signaling. Hepatology. 2011;54:2137–48.

High Levels of Hepatitis B Virus After the Onset of Disease Lead to Chronic Infection in Patients With Acute Hepatitis B

Hiroshi Yotsuyanagi,[1,a] Kiyoaki Ito,[2,5,a] Norie Yamada,[1,3,4] Hideaki Takahashi,[3] Chiaki Okuse,[3] Kiyomi Yasuda,[4] Michihiro Suzuki,[3] Kyoji Moriya,[1] Masashi Mizokami,[2] Yuzo Miyakawa,[6] and Kazuhiko Koike[1]

[1]Department of Internal Medicine, Graduate School of Medicine, University of Tokyo, Bunkyo; [2]The Research Center for Hepatitis and Immunology, National Center for Global Health and Medicine, Ichikawa; [3]Division of Gastroenterology and Hepatology, Department of Internal Medicine, St Marianna University School of Medicine, Kawasaki; and [4]Department of Internal Medicine, Center for Liver Diseases, Kiyokawa Hospital, Suginami, [5]Department of Microbiology and Immunology, Aichi Medical University School of Medicine, and [6]Miyakawa Memorial Research Foundation, Minato, Tokyo, Japan

Background. Some patients with acute hepatitis B virus (HBV) infection develop chronic infection. However, the method for identifying these patients has not been established.

Methods. We followed 215 Japanese patients with acute HBV infection until the clearance of hepatitis B surface antigen (HBsAg) or the development of chronic infection. Levels of HBsAg and HBV DNA were serially monitored from the onset.

Results. Of the 215 patients, 113 (52.5%) possessed HBV genotype A, 26 (12.0%) genotype B, and 73 (34.0%) genotype C. Twenty-one of the 215 (9.8%) developed chronic infection, with the persistence of HBsAg for >6 months. The rate of chronicity of genotype A, B, and C was 12.4%, 3.8%, and 8.2%. Of the 21 patients, only 6 (2.8%) patients, including 5 with genotype A, failed to clear HBsAg within 12 months. Levels of HBsAg at 12 weeks and HBV DNA at 4 weeks were useful for distinguishing the patients who became chronic from those who did not ($P < .001$ and $P < .001$, respectively). Likewise, the levels of HBsAg at 12 weeks and HBV DNA at 8 weeks were useful for discriminating between the patients who lost HBsAg within 12 months and those who did not ($P < .01$ and $P < .05$, respectively).

Conclusions. In acute HBV infection, clearance of HBV may happen between 6 and 12 months from the onset. Only those who fail to clear HBV within 12 months from the onset may develop chronic infection.

Keywords. hepatitis B virus antigen; hepatitis B virus; genotype.

The clinical outcome of acute hepatitis B is self-limited in the majority of immunocompetent adults. However, some patients run a prolonged or even chronic course, or are complicated by acute liver failure. Several factors are implicated in different clinical courses.

Hepatitis B virus (HBV) genotypes and subtypes are known to influence the clinical outcome of acute hepatitis B. For instance, HBV subgenotype B1 is associated with fulminant hepatic failure in acute hepatitis B [1]. On the other hand, genotype A is associated with chronic sequelae [2–5]. Furthermore, patients with subgenotype C2 are more likely to develop chronic infection than those with subgenotype B2 [6]. These characteristics may reflect viral kinetics in acute HBV infection that would differ among HBV infections with distinct genotypes/subgenotypes, but little is known about them.

Quantitation of hepatitis B surface antigen (HBsAg), in addition to HBV DNA, has been introduced to analysis of viral kinetics in patients with chronic hepatitis B in recent years. HBsAg levels are also useful for estimating

Received 14 February 2013; accepted 9 May 2013; electronically published 23 May 2013.

[a]H. Y. and K. I contributed equally to this work.

Correspondence: Hiroshi Yotsuyanagi, MD, Department of Internal Medicine, Graduate Institute of Medicine, University of Tokyo, 7-3-1, Hongo, Bunkyo, Tokyo 113-8655, Japan (hyotsu-tky@umin.ac.jp).

Clinical Infectious Diseases 2013;57(7):935–42

DOI: 10.1093/cid/cit348

viral loads and predicting the response to antiviral treatments [7–9], and for determining the natural history of chronic hepatitis B [10, 11]. Therefore, HBsAg and HBV DNA would be instrumental in foretelling the outcome of acute hepatitis B. However, the clinical utility of these markers in patients with acute hepatitis B is largely unknown.

Therefore, the aim of the present study was to examine differences in viral kinetics among patients with acute hepatitis B, who were infected with HBV of different genotypes, and evaluate the usefulness of quantifying HBsAg and HBV DNA for predicting the clinical outcome.

PATIENTS AND METHODS

Patients

This was a retrospective study of patients who were diagnosed with acute hepatitis B in our institutions during 1994 through 2010. Criteria for the diagnosis of acute hepatitis B were (1) acute onset of liver injury without a previous history of liver dysfunction; (2) detection of HBsAg in the serum; (3) immunoglobulin M (IgM) antibody to HBV core (anti-HBc) in high titers (detectable in serum samples diluted 10-fold) [3]; (4) absence of a past or family history of chronic HBV infection; and (5) exclusion of coinfection with hepatitis A virus, hepatitis C virus, or other hepatotropic viruses by serologic testing. Among the 232 patients who met these criteria, 215 patients (159 men and 56 women with a mean age of 31.8 ± 10.0 years) whose serum samples were available for virologic analyses were included in the study. No patient developed liver failure.

No patient received antiviral treatment. Of the 215 patients, 159 (74.0%) patients could be regularly followed up until the confirmation of clinical outcomes. Based on the duration of HBsAg (defined as the interval between the onset [defined by the first visit] and the last visit with detectable HBsAg), we classified the 159 patients into the following 4 groups (the duration of HBsAg is indicated in parentheses): group 1 (<3 months); group 2 (3–6 months); group 3 (>6–12 months); and group 4 (>12 months). Changes in virologic parameters were analyzed in relation with clinical characteristics. The study was approved by the ethics committees of our institutions, and written informed consent was obtained from each patient.

Quantification of Serologic Markers for HBV Infection and HBV DNA

HBsAg had been measured quantitatively by chemiluminescent enzyme-linked immunosorbent assay (ELISA; Sysmex JAPAN Co, Ltd, Kobe, Japan) every 2–4 weeks, until the clinical outcome was known. It has a dynamic range of 0.03–2, 500 IU/mL. Serum samples scaling out from this range were diluted so as to contain them within it. Antibody to hepatitis B s antigen (anti-HBs), hepatitis B e antigen (HBeAg), and IgM anti- HBc were determined by ELISA (Abbott JAPAN Co, Ltd, Tokyo, Japan). Levels of HBV DNA were determined using the COBAS TaqMan HBV v.2.0 kit (Roche Diagnostics, Basel, Switzerland), which has a dynamic range over 2.1–9.0 log copies/mL.

HBV Genotyping

The HBV genotype was determined by a genotype-specific probe assay (Smitest HBV genotyping Kit, Genome Science, Fukushima, Japan) as previously reported [12].

Molecular Evolutionary Analyses

HBV genotype A started to prevail in Japan merely several years ago, suggesting that it was imported to Japan only recently [3, 13]. Therefore, genomic sequences of HBV genotype A (HBV/A), recovered from sera of patients with acute HBV infection, would be closely related to one another and with those reported from abroad. To evaluate this possibility, 20 HBV/A samples were selected randomly and sequenced by the method reported previously [14].

The number of nucleotide substitutions per site was estimated by the 6-parameter method [15], and a phylogenetic tree was constructed by the neighbor-joining method [16] based on the numbers of substitutions. To confirm the credibility of phylogenetic analyses, bootstrap resampling tests were carried out 1000 times [17].

Statistical Analyses

Categorical variables were compared by χ^2 test or Fisher exact test, and continuous variables by the Mann-Whitney U test. $P < .05$ was considered statistically significant. Receiver operating characteristic (ROC) analysis was performed to compute the area under the ROC curves for viral markers to determine cutoff points for predicting the outcome.

RESULTS

Distribution of HBV Genotypes in Patients With Acute Hepatitis B

HBV genotypes were determined in 215 of the 232 (93%) patients with acute hepatitis B. Of the 215 patients, genotype A was detected in 113 (52%), B in 26 (12%), C in 73 (33%), D in 1 (1%), E in 1 (1%), and F in 1 (1%). The distribution of genotypes was compared among 4 periods during 1994 through 2010 (Table 1). The proportion of patients with genotype A gradually increased to 65.9% in 2007–2010; it was higher than those in the earlier periods (34.4% in 1994–1998 [$P = .002$], 36.8% in 1999–2002 [$P = .002$], and 51.9% in 2003–2006 [$P = .093$]).

Phylogenetic Relationship Among HBV Strains of Genotype A

We randomly selected 11 HBV/A strains sampled in 2007–2010 and 9 of those in 2001–2006, and constructed a molecular evolutionary tree (Figure 1). All 20 samples had similar nucleotide sequences with a concordance of 99%. They were close to previously

Table 1. Prevalence of Hepatitis B Virus Genotypes in Patients With Acute Hepatitis B During 4 Chronologic Periods

Period	Genotype A	Genotype B	Genotype C	Others
1994–1998 (n = 32)	11[a] (34.4%)	3 (9.3%)	18 (56.3%)	0
1994–1998 (n = 38)	14[b] (36.8%)	4 (10.5%)	20 (52.7%)	0
1994–1998 (n = 54)	28[c] (51.9%)	6 (11.1%)	19 (35.1%)	1 (1.9%)
1994–1998 (n = 91)	60[a,b,c] (65.9%)	13 (14.3%)	16 (17.6%)	2 (2.2%)
Total (N = 215)	113 (52.5%)	26 (12.0%)	73 (34.0%)	3 (1.5%)

[a] $P = .0032$.

[b] $P = .0014$.

[c] $P = .02$.

reported genotype A2 sequences from Western countries. The results support the possibility that HBV/A was imported to Japan only recently and has been spreading throughout the country.

Clinical Features Among Patients Infected With HBV of Different Genotypes

Clinical features of patients with acute hepatitis B of different genotypes are compared in Table 2. The mean age was no different among patients infected with HBV of different genotypes. The proportion of men was higher in genotype A or B than C infection (93.8% or 80.7% vs 39.7% [A vs C, $P < .001$; B vs C, $P < .001$]).

The maximum alanine aminotransferase (ALT) level was lower in patients with genotype A than in those with genotype C (2126 ± 938 vs 2857 ± 1668 IU/L, $P = .002$). The maximum bilirubin level was higher in patients with genotype A (7.1 ± 6.4 mg/dL) or C (9.0 ± 7.5 mg/dL) than in those with genotype B (4.8 ± 3.3 mg/dL) (A vs B, $P = .003$; B vs C, $P < .001$). Regarding viral markers, the peak HBV DNA level was higher in patients with genotype A than in those with genotype C (6.3 ± 1.7 vs 4.9 ± 1.5 log copies/mL, $P < .001$). HBeAg was detected in 95 of the 121 (77.3%) patients with genotype A, 24 of the 28 (88.5%) with genotype B, and 37 of the 58 (65.5%) with genotype C (A vs C, $P = .036$). Men who have sex with men were more frequently represented among patients with genotype A than B or C (31.4% vs 4.8% or 11.3% [A vs B, $P = .017$; A vs C, $P = .002$]). Antibody to human immunodeficiency virus (anti-HIV) was examined in 72 of the 113 (63.7%) patients with genotype A, 7 of the 26 (26.9%) with genotype B, 58 of the 73 (79.5%) with genotype C, and 1 with genotype E. Anti-HIV was detected in 7 of the 72 (9.7%) patients with genotype A, and the other 96 patients tested for anti-HIV showed negative results. All of the 7 patients with anti-HIV cleared HBsAg from the serum within 6 months without antiviral treatment.

Among the 215 patients whose HBV genotypes were determined, 159 could be followed until the confirmation of clinical outcomes. The distribution of HBsAg-positive period is compared among patients with different genotypes. Group 1 (HBsAg persisting for <3 months) comprised 84 patients; group 2 (3–6 months) comprised 54 patients; group 3 (>6–12 months) comprised 15 patients; and group 4 (>12 months) comprised 6 patients. HBsAg remained >6 months in 21 of the 215 (9.8%) patients, including 14 of the 113 (12.4%) with genotype A, 1 of the 26 (3.8%) with genotype B, and 6 of the 73 (8.2%) with genotype C. Among the 21 patients, 15 (71.4%) cleared HBsAg within 12 months from the onset, and were classified into group 3. The remaining 6 (5 with genotype A and 1 with genotype B) who failed to clear HBsAg within 12 months were classified into group 4. All of the 6 were negative for anti-HIV. The proportion of group 4 was 6.0% in the patients with genotype A, 4.0% in those with genotype B, and 0% in those with genotype C.

The mean duration of HBsAg was 13.9 ± 8.7 weeks in patients with genotype A, 7.1 ± 5.3 weeks in those with genotype B, and 9.6 ± 7.6 weeks in those with genotype C, presuming the duration of HBsAg in group 4 at 12 months. The duration was longer in patients with genotype A than in those with B or C (A vs B, $P < .001$; A vs C, $P = .04$).

Prediction of the Outcome by the Duration of HBsAg

Table 2 shows that the duration of HBsAg among patients with genotype A varied to a higher extent than that among those with other genotypes. Therefore, we determined HBsAg and HBV DNA levels serially, and evaluated them for the ability to predict the outcome of acute hepatitis B in patients with genotype A.

Serial changes in HBsAg levels are shown in Supplementary Figure 1*A*. HBsAg levels declined more slowly in group 2 than group 1, as well as in group 3 than group 2. In group 4, HBsAg reelevated at 12 weeks after the onset. Figure 2 compares HBsAg levels among groups 1–4 at different intervals from the onset. HBsAg at 8 weeks from the onset was useful for distinguishing group 3 or 4 from group 1 or 2. Likewise, HBsAg at 12 weeks from the onset was helpful for discriminating among groups 2, 3, and 4.

Prediction of the Outcome by HBV DNA

We also studied serial changes of HBV DNA in patients with genotype A, and examined if they also were useful for predicting the clinical outcome of acute hepatitis B. Supplementary Figure 1*B* shows serial changes in HBV DNA levels in patients in 4 groups. Although the reelevation of HBV DNA was not observed, the decline of HBV DNA was quite slow in group 4. Figure 3 compares HBV DNA levels among groups 1–4 at different intervals from the onset. HBV DNA at 4 weeks from

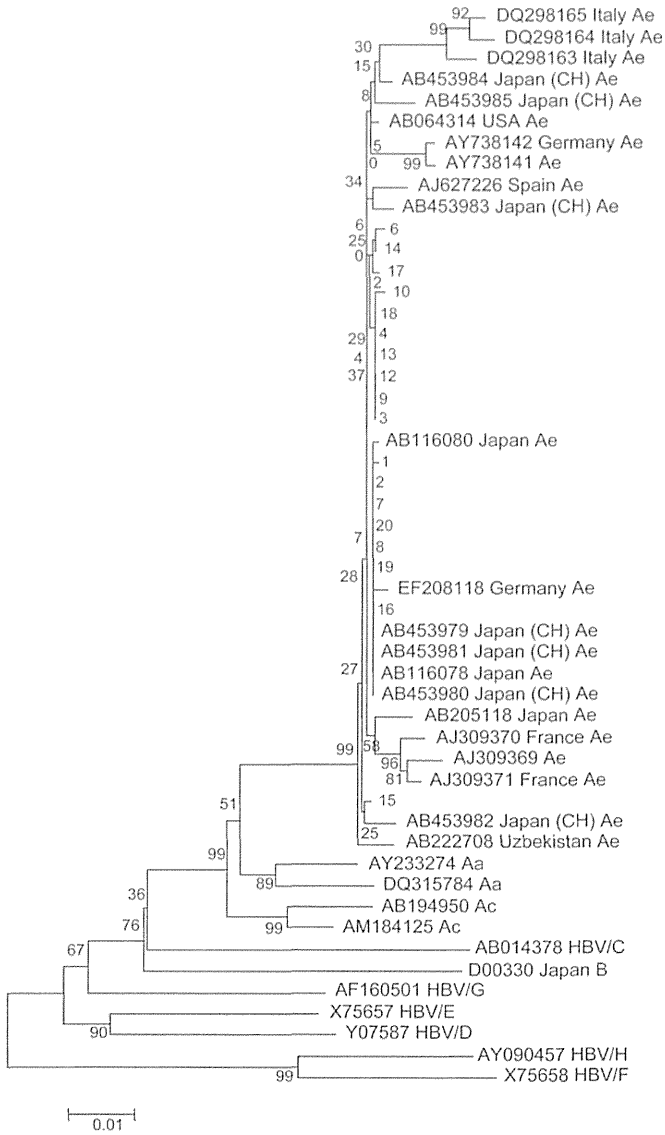

Figure 1. Evolutionary relationships of 86 hepatitis B virus genotype A taxa, including 20 from the present cases. The evolutionary history, inferred using the neighbor-joining method, shows that all 20 samples had similar nucleotide sequences close to previously reported genotype A2 sequences from Western countries.

the onset was useful for distinguishing group 3 or 4 from group 1 or 2. Likewise, HBV DNA levels at 8 weeks from the onset were useful for discriminating between group 4 and group 3, as well as for distinguishing group 3 or 4 from group 1 or 2.

Levels of HBsAg and HBV DNA for Predicting Persistent Infection

As the levels of HBsAg at 12 weeks and HBV DNA at 8 weeks from the onset were useful for distinguishing group 4 from the other groups, we evaluated the appropriate levels for predicting persistent infection in patients with genotype A. When we set the cutoff value of HBsAg at 1000 IU/mL based on the ROC analysis, both the positive predictive value and the negative predictive value were 100% with high sensitivity (100%) and specificity (98.1%). Likewise, when we set the cutoff value of HBV DNA at 10^6 log IU/mL based on the ROC analysis, both the positive predictive value and the negative predictive value were 100% with high sensitivity (100%) and specificity (96.4%). Therefore, HBsAg at 12 weeks >1000 IU/mL or HBV DNA at 8 weeks >10^6 log copies/mL is useful for predicting persistent infection.

DISCUSSION

In Japan, as shown in Table 1, the dominant HBV in acute hepatitis has been shifting from genotype C to A [3, 5, 14, 18]. The fact that nucleotide sequences of HBV/A isolates from patients

Table 2. Baseline Characteristics and the Duration of Hepatitis B Surface Antigen in Patients With Acute Hepatitis B Virus With Different Hepatitis B Virus Genotypes

	HBV Genotypes					
Features	A (n = 113)	B (n = 26)	C (n = 73)	D (n = 1)	E (n = 1)	F (n = 1)
Age, y	30.8 ± 9.5	32.3 ± 9.5	33.3 ± 10.9	27	26	58
Male	106 (93.8%)[a]	21 (80.7%)[b]	29 (39.7%)[a,b]	0	0	1 (100%)
Transmission routes Identified	102 (90.2%)	21 (80.8%)	53 (72.6%)	1 (100%)	1 (100%)	1 (100%)
Heterosexual	70 (68.6%)	19 (90.4%)	47 (88.7%)	1 (100%)	1 (100%)	1 (100%)
MSM	32 (31.4%)[c,d]	1 (4.8%)[c]	6 (11.3%)[d]	0	0	0
ALT, IU/L	2126 ± 938[e,*]	2394 ± 820	2857 ± 1668[e]	4180	1175	1533
Bilirubin, mg/dL	7.1 ± 6.4[f*]	4.8 ± 3.3[f,g]	9.0 ± 7.5[g]	6.8	3.9	3.5
HBV DNA, log copies/mL	6.3 ± 1.7[h,*]	5.5 ± 2.3	4.9 ± 1.5[h]	5.2	7.4	4.8
HBeAg	95/121 (77.3%)[i,*]	24/28 (88.5%)	37/58 (65.5%)[i]	1/1 (100%)	1/1 (100%)	1/1 (100%)
Anti-HIV	7/72 (9.7%)	0/7 (0%)	0/23 (0%)	Not tested	0/1 (0%)	Not tested
Duration of HBsAg*						
Group (mo)						
1 (<3)	35 (42.2%)	16 (64.0%)	31 (64.6%)	0	1	1
2 (3–6)	34 (41.0%)	8 (32.0%)	11 (22.9%)	1	0	0
3 (>6 –12)	9 (10.8%)	0	6 (12.5%)	0	0	0
4 (>12)	5 (6.0%)	1 (4.0%)	0	0	0	0

Abbreviations: ALT, alanine aminotransferase; anti-HIV, antibody to human immunodeficiency virus; HBeAg, hepatitis B e antigen; HBsAg, hepatitis B surface antigen; HBV, hepatitis B virus; MSM, men who have sex with men.

[a] $P < .001$.

[b] $P < .001$.

[c] $P = .017$.

[d] $P = .002$.

[e] $P = .002$.

[f] $P = .003$.

[g] $P < .001$.

[h] $P < .001$.

[i] $P = .036$.

* Data from anti-HIV-positive patients are excluded.

with acute hepatitis B in this study were very close to one another suggests that most HBV/A strains were imported recently and have spread rapidly, which may be attributed to the features of HBV/A in transmission routes and viral kinetics. We have reported that patients with genotype A tend to have multiple sexual partners [5]. Consequently, chances of secondary transmission of HBV/A would be higher than those of other genotypes, which may increase the number of patients who contract HBV/A infections. On the other hand, HBsAg persisted longer in patients with genotype A than B or C, which is consistent with the in vivo experiment using chimera mice carrying human hepatocytes showing that proliferation of HBV starts later and lasts longer in genotype A than in B or C infection [19].

Our results have shown that 6% of the patients with genotype A develop persistent infection. Because liver cirrhosis or hepatocellular carcinoma can develop in a substantial population of HBV carriers [20, 21], it is important to distinguish the patients in whom HBV infection becomes chronic, and follow them carefully. Although polymorphisms in host genes may be useful for identifying patients who are prone to develop chronic HBV infection [22], simple surrogate markers for the outcome have not been reported. Our data indicate that it would be difficult to predict the clinical outcome based on serum levels of viral markers at the first visit alone. This is understandable, because the dose of infecting virus, as well as the interval between infection and the first visit, can vary widely. Hence, we set out to analyze changes in serum levels of viral markers.

As seen in Figure 2, HBsAg levels at 12 weeks from the onset were most useful for discriminating among groups 2, 3, and 4 in the genotype A infection. Therefore, the outcome of acute hepatitis B may be predictable at this time point. Of note is the reelevation of HBsAg observed in group IV (Supplementary Figure 1*A*). Reelevation of viral markers suggests prolonged viral proliferation in the liver, and may be useful to identify the patients who may develop chronic infection.

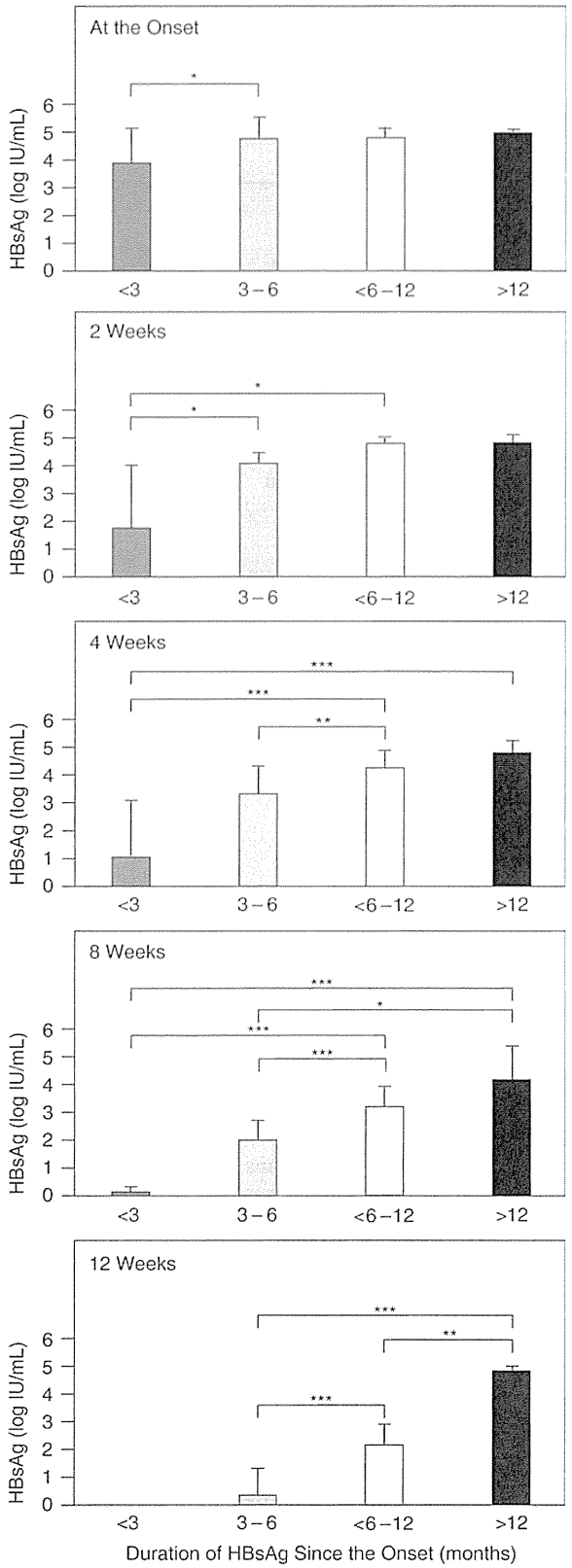

Figure 2. Levels of hepatitis B surface antigen in patients with different durations of infection compared at various weeks after the onset of acute hepatitis B genotype A *P < .05; **P < .01; ***P < .001. Abbreviation: HBsAg, hepatitis B surface antigen.

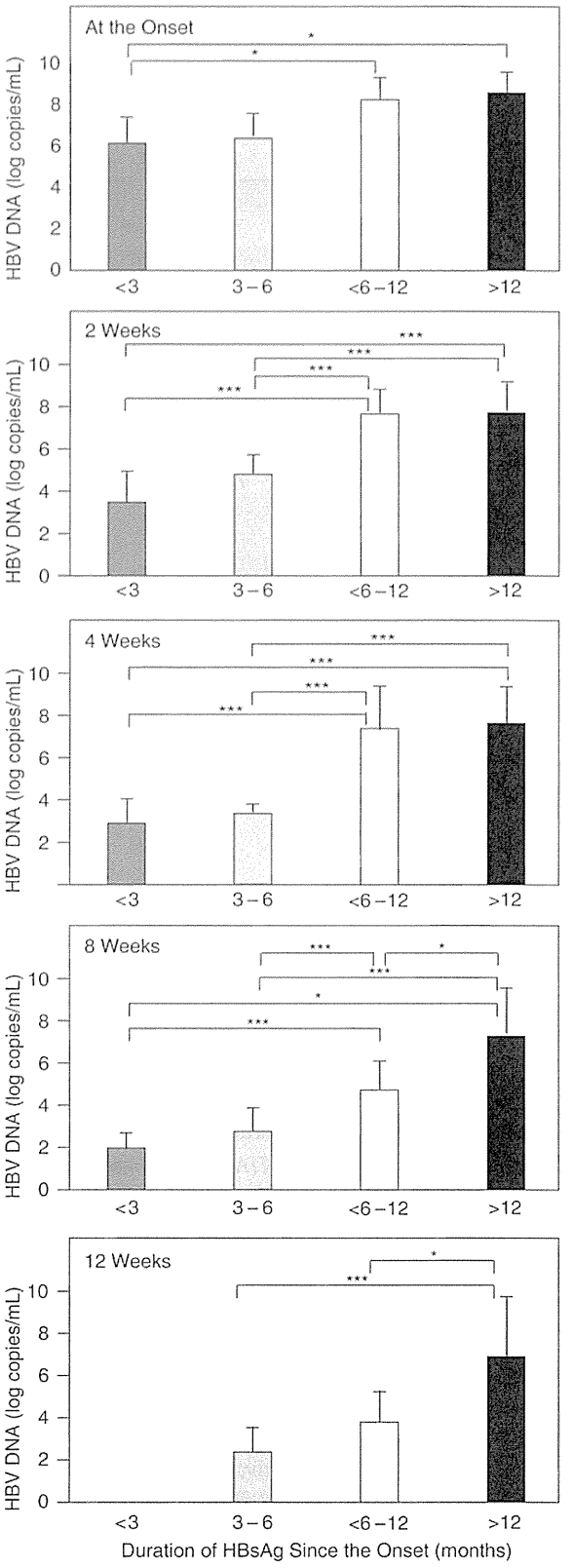

Figure 3. Levels of hepatitis B virus DNA in patients with different durations of infection compared at various weeks after the onset of acute hepatitis B genotype A. *P < .05; **P < .01; ***P < .001. Abbreviations: HBsAg, hepatitis B surface antigen; HBV, hepatitis B virus.

As shown in Figure 3, HBV DNA levels at 4 weeks from the onset can discriminate groups 1/2 from groups 3/4. Furthermore, HBV DNA levels at 8 weeks from the onset can distinguish group 4 from group 1, 2, or 3. Therefore, the combination of HBV DNA levels at weeks 4 and 8 would be useful for predicting the outcome. For the prediction of a chronic outcome, HBV DNA level at 8 weeks from the onset is a useful surrogate marker of the outcome as well as HBsAg level at 12 weeks. There were differences in viral kinetics among groups 1, 2, 3, and 4.

Our present study showed that 15 of the 215 patients (7.0%) cleared HBsAg from >6 to 12 months after the onset. Sixty percent of the 15 patients had HBV/A. Although these patients met the criteria of chronic infection, they finally cleared HBsAg from the sera. Therefore, we would like to propose that transition to chronic infection in acute hepatitis B be judged at 12 months from onset in patients with genotype A; further studies in larger cohorts are necessary. One reason for our proposal is the indication of antiviral treatment. Antiviral treatment in patients with acute hepatitis B is not indicated because previous studies failed to show the efficacy of antiviral treatments in the patients with acute hepatitis B [23, 24]. However, if patients who actually develop chronic infection can be identified and treated by antiviral treatment, the number of those who develop secondary infection may be markedly reduced. Evaluation of the efficacy of antiviral treatments by prospective studies, based on surrogate markers for the outcome, should be conducted as the next step. HBeAg, which was reported to be useful as a surrogate marker for chronicity, should also be assessed as a surrogate marker [25, 26].

Our study has some limitations. First, the lack of data in early stages made it difficult to study viral kinetics precisely. Second, viral kinetics in the infection with each HBV genotype were obtained from a restricted number of patients, not large enough to establish the usefulness of changes in viral markers in earlier stages of HBV infection. Third, anti-HIV was not checked in all patients due to the lack of informed consent. Fourth, HBsAg and HBV DNA were not determined 24 weeks after onset when discrimination between groups 3 and 4 may be possible more easily. Fifth, the maximum levels of ALT and bilirubin may be affected by the time of blood test. Validation studies in larger cohorts are necessary to evaluate the feasibility of our hypotheses.

In conclusion, we have shown that viral kinetics and the clinical outcome are different among patients with acute hepatitis B who are infected with HBV of distinct genotypes. HBsAg levels at 12 weeks and HBV DNA at 8 weeks after the onset would be useful to predict the clinical outcome of patients with acute hepatitis B.

Supplementary Data

Supplementary materials are available at *Clinical Infectious Diseases* online (http://cid.oxfordjournals.org/). Supplementary materials consist of data provided by the author that are published to benefit the reader. The posted materials are not copyedited. The contents of all supplementary data are the sole responsibility of the authors. Questions or messages regarding errors should be addressed to the author.

Notes

Financial support. This work was supported by grants from the Ministry of Health, Labor and Welfare of Japan.

Potential conflicts of interest. All authors: No reported conflicts.

All authors have submitted the ICMJE Form for Disclosure of Potential Conflicts of Interest. Conflicts that the editors consider relevant to the content of the manuscript have been disclosed.

References

1. Kusakabe A, Tanaka Y, Mochida S, et al. Case-control study for the identification of virological factors associated with fulminant hepatitis B. Hepatol Res **2009**; 39:648–56.
2. Mayerat C, Mantegani A, Frei PC. Does hepatitis B virus (HBV) genotype influence the clinical outcome of HBV infection? J Viral Hepat **1999**; 6:299–304.
3. Tamada Y, Yatsuhashi H, Masaki N, et al. Hepatitis B virus strains of subgenotype A2 with an identical sequence spreading rapidly from the capital region to all over Japan in patients with acute hepatitis B. Gut **2012**; 61:765–73.
4. Kobayashi M, Arase Y, Ikeda K, et al. Clinical features of hepatitis B virus genotype A in Japanese patients. J Gastroenterol **2003**; 38:656–62.
5. Yotsuyanagi H, Okuse C, Yasuda K, et al. Distinct geographic distributions of hepatitis B virus genotypes in patients with acute infection in Japan. J Med Virol **2005**; 77:39–46.
6. Zhang HW, Yin JH, Li YT, et al. Risk factors for acute hepatitis B and its progression to chronic hepatitis in Shanghai, China. Gut **2008**; 57: 1713–20.
7. Reijnders JG, Rijckborst V, Sonneveld MJ, et al. Kinetics of hepatitis B surface antigen differ between treatment with peginterferon and entecavir. J Hepatol **2011**; 54:449–54.
8. Sonneveld MJ, Rijckborst V, Boucher CA, Hansen BE, Janssen HL. Prediction of sustained response to peginterferon alfa-2b for hepatitis B e antigen-positive chronic hepatitis B using on-treatment hepatitis B surface antigen decline. Hepatology **2010**; 52:1251–7.
9. Wursthorn K, Jung M, Riva A, et al. Kinetics of hepatitis B surface antigen decline during 3 years of telbivudine treatment in hepatitis B e antigen-positive patients. Hepatology **2010**; 52:1611–20.
10. Brunetto MR, Oliveri F, Colombatto P, et al. Hepatitis B surface antigen serum levels help to distinguish active from inactive hepatitis B virus genotype D carriers. Gastroenterology **2010**; 139:483–90.
11. Jaroszewicz J, Calle Serrano B, Wursthorn K, et al. Hepatitis B surface antigen (HBsAg) levels in the natural history of hepatitis B virus (HBV) infection: a European perspective. J Hepatol **2010**; 52:514–22.
12. Kato H, Orito E, Sugauchi F, et al. Frequent coinfection with hepatitis B virus strains of distinct genotypes detected by hybridization with type-specific probes immobilized on a solid-phase support. J Virol Methods **2003**; 110:29–35.
13. Yano K, Tamada Y, Yatsuhashi H, et al. Dynamic epidemiology of acute viral hepatitis in Japan. Intervirology **2010**; 53:70–5.
14. Matsuura K, Tanaka Y, Hige S, et al. Distribution of hepatitis B virus genotypes among patients with chronic infection in Japan shifting toward an increase of genotype A. J Clin Microbiol **2009**; 47:1476–83.
15. Gojobori T, Ishii K, Nei M. Estimation of average number of nucleotide substitutions when the rate of substitution varies with nucleotide. J Mol Evol **1982**; 18:414–23.
16. Saitou N, Nei M. The neighbor-joining method: a new method for reconstructing phylogenetic trees. Mol Biol Evol **1987**; 4:406–25.
17. Felsenstein J. Confidence limits on phylogenesis, an approach using the bootstrap. Evolution **1985**; 39:783–91.

18. Ogawa M, Hasegawa K, Naritomi T, Torii N, Hayashi N. Clinical features and viral sequences of various genotypes of hepatitis B virus compared among patients with acute hepatitis B. Hepatol Res **2002**; 23: 167–77.
19. Sugiyama M, Tanaka Y, Kurbanov F, et al. Direct cytopathic effects of particular hepatitis B virus genotypes in severe combined immunodeficiency transgenic with urokinase-type plasminogen activator mouse with human hepatocytes. Gastroenterology **2009**; 136:652–62. e3.
20. McMahon BJ, Holck P, Bulkow L, Snowball M. Serologic and clinical outcomes of 1536 Alaska Natives chronically infected with hepatitis B virus. Ann Intern Med **2001**; 135:759–68.
21. Chu CM. Natural history of chronic hepatitis B virus infection in adults with emphasis on the occurrence of cirrhosis and hepatocellular carcinoma. J Gastroenterol Hepatol **2000**; 15(suppl):E25–30.
22. Kamatani Y, Wattanapokayakit S, Ochi H, et al. A genome-wide association study identifies variants in the HLA-DP locus associated with chronic hepatitis B in Asians. Nat Genet **2009**; 41:591–5.
23. Kumar M, Satapathy S, Monga R, et al. A randomized controlled trial of lamivudine to treat acute hepatitis B. Hepatology **2007**; 45:97–101.
24. Tassopoulos NC, Koutelou MG, Polychronaki H, Paraloglou-Ioannides MHadziyannis SJ. Recombinant interferon-alpha therapy for acute hepatitis B: a randomized, double-blind, placebo-controlled trial. J Viral Hepat **1997**; 4:387–94.
25. Aldershvile J, Frösner GG, Nielsen JO, et al. Hepatitis B e antigen and antibody measured by radioimmunoassay in acute hepatitis B surface antigen-positive hepatitis. J Infect Dis **1980**; 141:293–8.
26. Aldershvile J, Nielsen JO. HBeAg, anti-HBe and anti-HBc IgM in patients with hepatitis B. J Virol Methods **1980**; 2:97–105.

Biochemical and Biophysical Research Communications 438 (2013) 230–235

Contents lists available at ScienceDirect

Biochemical and Biophysical Research Communications

journal homepage: www.elsevier.com/locate/ybbrc

Inhibition of microRNA122 decreases SREBP1 expression by modulating suppressor of cytokine signaling 3 expression

Chikako Shibata [a], Takahiro Kishikawa [a], Motoyuki Otsuka [a,b,*], Motoko Ohno [a], Takeshi Yoshikawa [a], Akemi Takata [a], Haruhiko Yoshida [a], Kazuhiko Koike [a]

[a] Department of Gastroenterology, Graduate School of Medicine, The University of Tokyo, Tokyo 113-8655, Japan
[b] Japan Science and Technology Agency, PRESTO, Kawaguchi, Saitama 332-0012, Japan

ARTICLE INFO

Article history:
Received 13 July 2013
Available online 24 July 2013

Keywords:
microRNA
Liver
SOCS3
SREBP
Expression regulation

ABSTRACT

While inhibition of microRNA122 (miR122) function *in vivo* results in reduced serum cholesterol and fatty acid levels, the molecular mechanisms underlying the link between miR122 function and lipid metabolism remains unclear. Because the expression of SREBP1, a central transcription factor involved in lipid metabolism, is known to be increased by suppressor of cytokine signaling 3 (SOCS3) expression, and because we previously found that SOCS3 expression is regulated by miR122, in this study, we examined the correlation between miR122 status and the expression levels of SOCS3 and SREBP1. SREBP1 expression decreased when SOCS3 expression was reduced by miR122 silencing *in vitro*. Conversely, SREBP1 expression in miR122-silenced cells was restored by enforced expression of SOCS3. Such correlations were observed in human liver tissues with different miR122 expression levels. These signaling links may explain one of the molecular mechanisms linking inhibition of miR122 function or decreased expression of miR122 to decreased fatty acid and cholesterol levels, in the inhibition of miR122 function, or in pathological status in chronic liver diseases.

1. Introduction

MiRNA122 (miR122) is the most abundant and tissue-specific miRNA in the liver [1], and inhibition of miR122 *in vivo* was shown to greatly reduce serum cholesterol and fatty acid levels [2–6]. Recently, miravirsen, a locked nucleic acid-modified DNA phosphorothioate antisense oligonucleotide against miR122, was introduced practically to reduce hepatitis C virus (HCV) RNA levels in patients with HCV infection [7]. Although the primary purpose of the trial was to inhibit HCV replication, lipid levels were also found to decrease [7]. Despite consistent results concerning miR-122-mediated lipid metabolism, the underlying molecular mechanisms remain unclear, and although the expression levels of genes associated with lipid metabolism were affected by miR-122 inhibition, these genes were not direct targets of miR122, as judged by sequence similarities.

Members of the family of sterol regulatory element-binding proteins (SREBPs) are critical regulators of cholesterol and lipid homeostasis. The SBEBP family belongs to the basic helix–loop–helix–leucine zipper (bHLH-zipper) family of transcription factors and comprises SREBP-1a, SREBP-1c, and SREBP-2. The SREBF-1 gene on chromosome 17p11.2 encodes SREBP-1a and SREBP-1c, which are generated as alternatively spliced variants. Increased SREBP activity causes cholesterol and fatty acid accumulation by activating the expression of more than 30 genes dedicated to the synthesis and uptake of cholesterol, fatty acids, triglycerides, and phospholipids, as well as the NADPH cofactor required for synthesis of these molecules [8], which increases lipid levels.

The promoter activities of SREBP1 are potently inhibited by activated STAT3 [9]. In addition, STAT3-mediated inhibition of SREBP1 expression was shown to be antagonized by co-expression of the SOCS3 protein [9]. Conversely, SOCS3 inhibition in the liver in obese mice subjected to antisense treatment was reported to completely normalize the increased expression of SREBP1, leading to dramatic amelioration of hyperlipidemia. These results indicate the importance of SOCS3 in regulating SREBP expression and subsequent lipid metabolism [9].

We recently reported that silencing miR122 in hepatocytes leads to decreased SOCS3 expression accompanied by hypermethylation of the SOCS3 promoter in a Dnmt1-independent manner [10]. In this study, we first assessed the correlated expression levels of SREBP1 in miR122-silenced and miR122 precursor-overexpressing cells. In addition, SREBP1 was recovered by enforced expression or inhibition of SOCS3 in miR122-modulated cells. We next confirmed the correlations among miR122, SOCS3, and SREBP

* Corresponding author. Address: Department of Gastroenterology, Graduate School of Medicine, The University of Tokyo, 5-3-1 Hongo, Bunkyo-ku, Tokyo 113-8655, Japan. Fax: +81 3 3814 0021.
E-mail address: otsukamo-tky@umin.ac.jp (M. Otsuka).

0006-291X/$ - see front matter © 2013 Elsevier Inc. All rights reserved.
http://dx.doi.org/10.1016/j.bbrc.2013.07.064

expression levels in human liver tissues in various pathological states with different miR122 expression levels [11]. Based on these analyses, we infer a molecular link between miR122 and lipid metabolism in miR122 inhibition and various liver pathological states.

2. Methods

2.1. Cells

The Huh7 and Hep3B human hepatocellular carcinoma cell lines were obtained from the Japanese Collection of Research Bioresources (JCRB, Osaka, Japan). Cells were maintained in Dulbecco's modified Eagle's medium (DMEM) supplemented with 10% fetal bovine serum.

2.2. Plasmids, viral production, and transduction

A miR122 precursor-expressing plasmid with a puromycin resistance gene (pCDH-miR122 with puro) and an H1 promoter-driven antisense miR122 stem–loop–stem RNA-expressing plasmid (pmiRZIP122 with puro) were constructed as described previously [10]. For double stable Hep3B cells with miR122 precursor and SOCS3 shRNA expression, a miR122 precursor with hygromycin resistance gene (pCDH-miR122 with hygro) was constructed by replacement of the puromycin resistance gene with a hygromycin resistant gene using the infusion method (Clontech, Mountain View, CA). SOCS3 shRNA-expressing lentiviral particles were purchased from Santa Cruz Biotechnology (Dallas, TX). An HA-SOCS3-expressing lentiviral construct with a neomycin resistance gene was constructed as described previously [10]. A pCDH control vector (System Biosciences, Mountain View, CA) was used as a negative control. Lentiviral particles, produced using pPACKH1 lentivector packaging plasmid mix (System Biosciences) according to the manufacturer's recommendations, were used as a negative control. Cells were transduced with lentiviruses using polybrene (EMD Millipore, Billerica, MA) and were then selected using puromycin.

2.3. Reporter plasmids, transient transfections, and luciferase assays

The reporter plasmids used for analysis of miR122 function were constructed as described previously [12]. Plasmid transfection was performed using FuGene6 Transfection Reagent (Boehringer Mannheim, Mannheim, Germany) according to the manufacturer's instructions. pGL4-TK, a control plasmid containing *Renilla reniformis* (sea pansy) luciferase under the control of the herpes simplex virus thymidine kinase promoter (Promega, Madison, WI), was used to determine transfection efficiency. Relative luciferase values were calculated by normalizing firefly luciferase activity values to sea pansy luciferase activity values to account for changes in transfection efficiency. Luciferase activity was measured using a Dual Luciferase Reporter Assay System (Promega) with a Lumat LB9507 luminometer (EG&G Berthold, Bad Wildbad, Germany).

2.4. Northern blotting of miRNAs

Northern blotting of miRNAs was performed as described previously [23]. Briefly, total RNA was extracted using TRIzol Reagent (Invitrogen, Carlsbad, CA). Ten micrograms of RNA was resolved in denaturing 15% polyacrylamide gels containing 7 M urea in 1× TBE and then transferred to a Hybond N+ membrane (GE Healthcare, Milwaukee, WI) in 0.25× TBE. Membranes were UV-cross-linked and prehybridized in hybridization buffer. Hybridization was performed overnight at 42 °C in ULTRAhyb-Oligo Buffer (Ambion, Austin, TX) containing a biotinylated probe specific for miR122 (tgg agt gtg aca atg gtg ttt g), antisense miR122 (caa aca cca ttg tca cac tcc a), or U6 (cac gaa ttt gcg tgt cat cct t), which had previously been heated at 95 °C for 2 min. Membranes were washed at 42 °C in 2× SSC containing 0.1% SDS, and the bound probe was visualized using a BrightStar BioDetect Kit (Ambion). A pre-stained RNA size marker for small RNA (BioDynamics Laboratory, Tokyo, Japan) was used to estimate band sizes. Blots were stripped by boiling in a solution containing 0.1% SDS and 5 mM EDTA for 10 min prior to rehybridization.

2.5. Western blot analysis and antibodies

Western blotting was performed as described previously [12]. Anti-SREBP was purchased from Santa Cruz Biotechnology. Anti-β-actin was acquired from Sigma–Aldrich (St. Louis, MO). An anti-HA antibody was obtained from Roche Applied Science (Penzberg, Germany). Other antibodies were purchased from Cell Signaling Technology (Danvers, MA).

2.6. Immunohistochemistry

Tissue arrays containing liver tissues (LV1504) were purchased from US Biomax (Rockville, MD). Immunohistochemistry was performed as described previously [23]. Briefly, after deparaffinization of the slides, endogenous peroxidase activity was blocked with 3% hydrogen peroxide buffer. Antigen retrieval was achieved by incubating the slides at 89 °C in 10 mM sodium citrate buffer (pH 6.0) for 30 min. To minimize nonspecific background staining, slides were blocked in 5% normal goat serum (Dako, Glostrup, Denmark). Tissues were labeled overnight at 4 °C with primary antibodies raised against SOCS3 or SREBP1. Slides were then incubated with an anti-mouse horseradish peroxidase-conjugated secondary antibody (Nichirei Bioscience, Tokyo, Japan) for 1 h. Bound antibody was visualized by incubation in 3,3′-diaminobenzidine (Nichirei Bioscience) for 5 min. The slides were counterstained with hematoxylin, dehydrated with ethanol, and mounted using Clarion mounting medium (Biomeda, Foster City, CA).

2.7. In situ hybridization to assess miR122

Locked nucleic acid (LNA)-scramble (negative control), LNA-anti-U6 (positive control), and LNA-anti-miR122 probes were obtained from EXIQON (Vedbæk, Denmark). The expression of miR122 in liver tissues was examined by *in situ* hybridization as described previously [12]. Briefly, after deparaffinization, tissue sections were treated with 10 μg/ml proteinase K for 5 min at 37 °C, refixed with 4% paraformaldehyde, and acetylated with 0.25% anhydrous acetic acid in 0.1 M Tris–HCl buffer (pH 8.0). Following prehybridization for 30 min at 48 °C, hybridization was performed overnight with each LNA probe (20 nM) in hybridization buffer (5× SSC buffer, 50% formamide, 500 μg/ml tRNA, 50 μg/ml Cot-1 DNA). After the completion of hybridization, the sections were washed with 0.1× SSC buffer for 10 min at 52 °C three times and blocked with DIG blocking buffer (Roche Diagnostics, Basel, Switzerland) for 30 min. Sections were then probed with anti-DIG (1:500; Roche Diagnostics) for 1 h at room temperature. Detection was performed by incubation in NBT/BCIP buffer (Promega) overnight. Nuclei were stained with Nuclear Fast Red (Sigma–Aldrich).

2.8. Histological scoring

Tissue staining was scored as described previously [23]. Briefly, staining intensity was semiquantitatively categorized into the

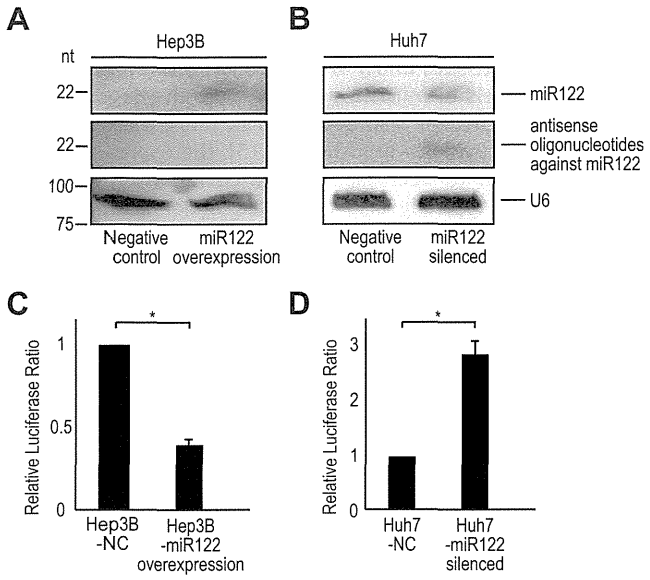

Fig. 1. Establishing of miR122-overexpressing and miR122-silenced cell lines. A, B, Northern blotting against miR122 and miR122 antisense oligonucleotides in Hep3B cells (A) and Huh7 cells (B). U6 levels were used as a loading control. Representative images from three independent experiments are shown. C, D, Luciferase expression from the reporter construct containing two tandem miR122 responsive elements in its 3'UTR, which are targeted by miR122, were examined. The suppressive effects of stably miR122 precursor-overexpressing Hep3B cells (C) and silencing effects on endogenous miR122 function in stably miR122 antisense-expressing Huh7 cells (D) are shown. Test values were normalized to those obtained from the cells transduced with a miRNA precursor-non-expressing negative control, which were set to 1 (nc). Data represent the mean ± standard deviations (SD) of three independent experiments.

following four categories by two independent investigators: –, no staining; +, weak staining; ++, moderate staining; and +++, intense staining. The color scale reflects staining intensity from green (no staining) to pink (intense staining).

2.9. Statistical analysis

Statistically significant differences between groups were determined using Student's *t*-test. *P*-values less than 0.05 were considered statistically significant.

3. Results

3.1. Establishment of miR122-overexpressing and -silenced cell lines

To determine the function of miR122, we modulated miR122 expression levels and function in liver cell lines by overexpressing an miR122 precursor construct or antisense sequences, respectively, against miR122, as previously reported [10,12]. Because Hep3B cells have relatively low miR122 expression and Huh7 cells have relatively high miR122 expression [13], we constructed miR122-overexpressing Hep3B cells and miR122-silenced Huh7 cells to examine the effects of modulating miR122. Overexpression of the miR122 precursor construct in Hep3B cells was confirmed by Northern blotting against miR122 sequences (Fig. 1A). Expression of the antisense construct against miR122 in Huh7 cells in Northern blotting appeared to be lower when using a probe to detect antisense miR122 (Fig. 1B). In these cells, miR122 levels were also lower, although miR122 was highly expressed in control Huh7 cells (Fig. 1B), suggesting that introduction of the antisense construct against miR122 may result not only in sequestration of endogenous miR122 by binding but also degradation of endogenous miR122 after formation of double-stranded RNA composed of sense and antisense miR122.

Next, we confirmed the changes in miR122 function using a luciferase reporter targeted by miR122. As predicted, in miR122-overexpressing Hep3B cells, luciferase activity decreased by more than half due to the ectopic miR122 expression (Fig. 1C). In contrast, in miR122-silenced Huh7 cells, luciferase activity increased about three times compared to control cells (Fig. 1D). These results suggest that modulation of miR122 by overexpressing exogenous constructs targeting miR122 was efficient.

3.2. SOCS3 and SREBP1 expression is decreased by miR122 silencing

Because we previously reported that miR122 silencing increased methylation in the promoter region of the SOCS3 gene and decreased its expression [10], we confirmed the expression levels of SOCS3 in miR122-overexpressing Hep3B cells and miR122-silenced Huh7 cells. Consistent with previous reports [10], SOCS3 expression increased and was downregulated in miR122-overexpressing Hep3B cells and miR122-silenced Huh7 cells, respectively (Fig. 2A and B). SOCS3 is a potent inhibitor of STAT3 activation [14]. Thus, we examined the phosphorylation status of STAT3. While total STAT3 expression levels remained unchanged, STAT3 phosphorylation decreased in miR122-overexpressing Hep3B cells and was higher in miR122-silenced Huh7 cells (Fig. 2A and B), suggesting that miR122 overexpression results in decreased STAT3 activation and that miR122 silencing has the opposite effect. Because a previous report revealed that STAT3 inhibits the promoter activity of SREBP1, a key regulator of fatty acid synthesis in the liver, we next examined the

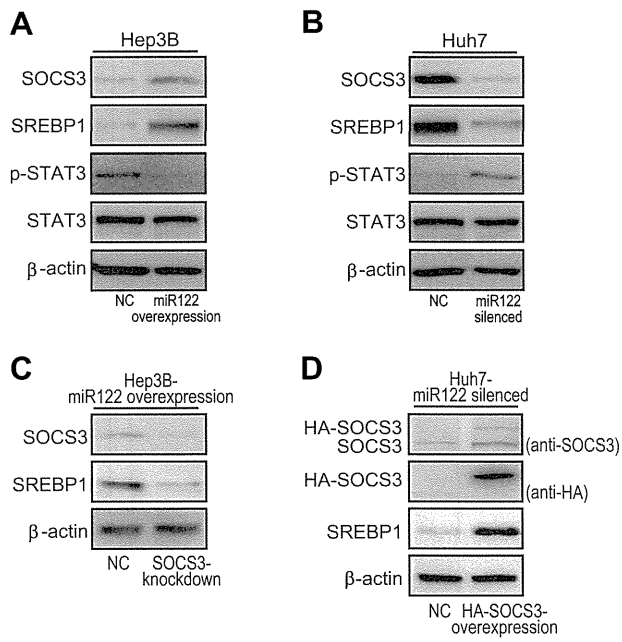

Fig. 2. SREBP1 expression is regulated by SOCS3. (A and B) SOCS3, SREBP1, and STAT3 protein expression levels and phosphorylation levels of STAT3 were determined by western blotting. Representative results from three independent experiments using Hep3B cells (A) and miR122-silenced Huh7 cells (B) are shown. (C) The effects of SOCS3 knockdown on SREBP expression in miR122 overexpressing Hep3B cell were stably transduced with SOCS3 shRNA. Representative results from three independent experiments are shown. (D) The effects of SOCS3 overexpression on SREBP expression in miR122-silenced Huh7 cells. Indicated protein expression levels were determined after miR122-silenced Huh7 cells were stably transduced with HA-SOCS3 expressing lentiviruses. HA-SOCS3 was visualized using anti-SOCS3 (the upper panel) and anti-HA (the second panel). Representative results from three independent experiments are shown.

expression levels of SREBP1 in miR122-modulated cells. The expression of SREBP1 was found to increase in miR122-overexpressing Hep3B cells and decrease in miR122-silenced Huh7 cells (Fig. 2A and B).

To confirm the role of OSCS3 in SREBP1 expression, we determined the effects of knockdown of SOCS3 expression in miR122-overexpresing Hep3B cells and enforced the expression of SOCS3 in miR122-silenced Huh7 cells (Fig. 2C and D). Knockdown of SOCS3 in miR122-overexpressing Hep3B cells reduced SREBP1 expression and enforced the expression of SOCS3 in miR122-silenced Huh7 cells increased SREBP1 expression (Fig. 2C and D). These results suggest that miR122 upregulates SOCS3 expression, resulting in the inhibition of STAT3 activation and subsequent upregulation of SREBP1 expression, and that inhibition of miR122 has the opposite effect.

3.3. Correlation of mIR122, SOCS3, and SREBP1 expression levels in human liver tissues

To confirm the above results in human clinical liver tissues, we examined 50 human liver tissues for the expression levels of miR122, SOCS3, and SREBP1 by *in situ* hybridization and immunohistochemistry (Fig. 3A and B). The expression levels of miR122 varied in liver tissues under various conditions (Fig. 3). When the expression levels of miR122 were reduced, the expression levels of SOCS3 and SREBP1 also decreased in more than 70% of cases (Fig. 3C). As previously reported [11,15], the expression levels of miR122 tended to decrease in liver cirrhosis, and SOCS3 and SREBP1 levels typically also decreased under such pathological conditions (Fig. 3C and Supplementary Table 1). These results may explain, at least in part, the decreased fatty acid and cholesterol synthesis observed clinically in the cirrhotic liver.

4. Discussion

In this study, we demonstrated that silencing miR122 function in liver cells resulted in decreased expression of SOCS3, and subsequently, decreased the expression of SREBP1. Because SREBP1 plays a key role in regulating fatty acid and cholesterol synthesis, reduced expression of miR122, which is frequently observed clinically in various chronic liver diseases [11,15], may be a cause of the decreased fatty acid and cholesterol synthesis in such pathological

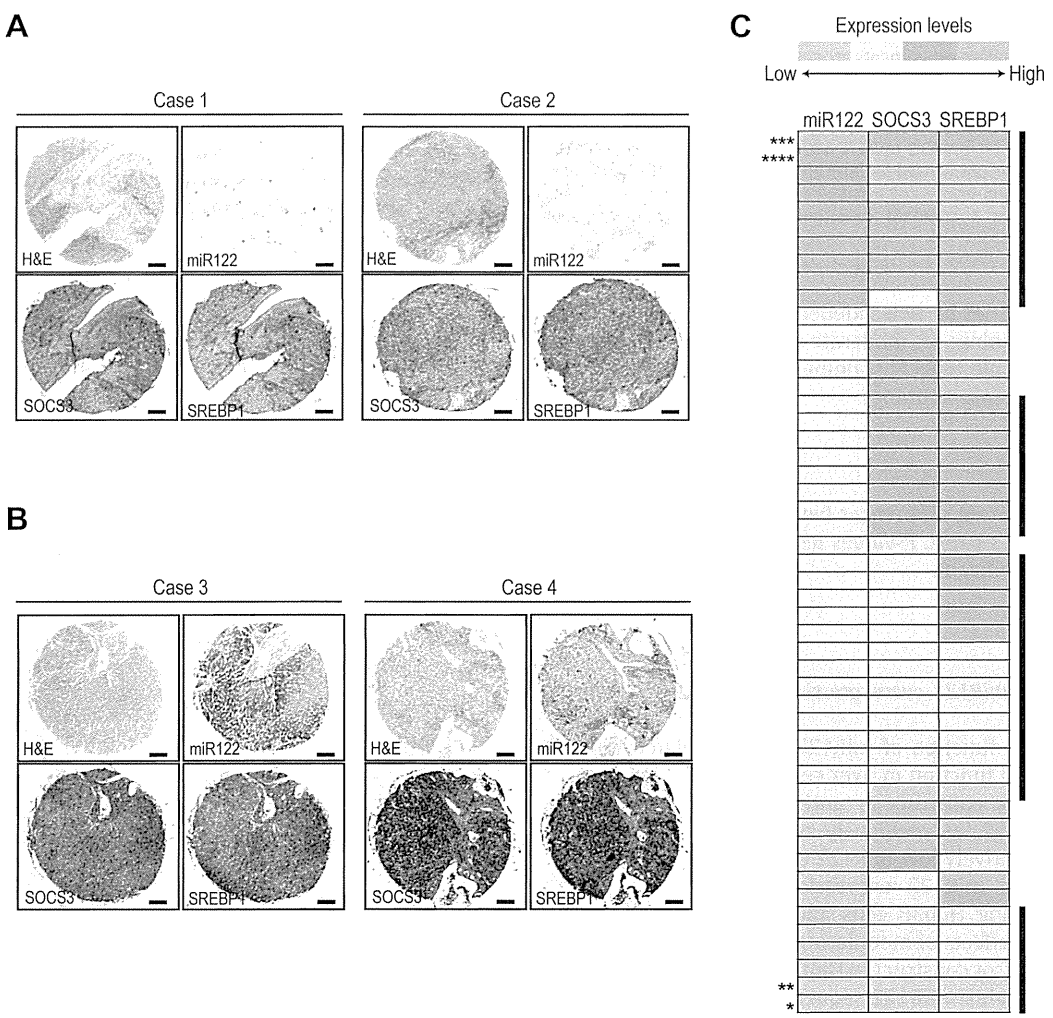

Fig. 3. Correlation of miR122, SOCS3, and SREBP expression levels in human liver tissues. (A and B), Representative liver tissues from four cases with correlated low (A) and high (B) expression levels of miR122, SOCS3, and SREBP. MiR122 was visualized by *in situ* hybridization (blue) and nuclei were stained with Nuclear Red (pink). SOCS3 and SREBP1 were stained by immunohistochemistry (brown). Bars, 500 μm. Hematoxylin and eosin (H&E)-stained tissues from each case are also shown as references. (C) Summarized expression levels of miR122, SOCS3, and SREBP1 in liver tissues from 50 cases. The color reflects the expression level of each parameter examined. Green denotes the lowest expression level and pink the highest, as the color scale bar at the top indicates. In 37 cases (indicated by black bars to the right), the differences between the expression scores of the three parameters are within one point on the color scale. *, Case 1 (A); **, Case 2 (A); ***, Case 3 (B); ****, Case 4 (B). (For interpretation of the references to color in this figure legend, the reader is referred to the web version of this article.)

states. In addition, silencing miR122 function decreases cholesterol and fatty acid levels [2–7]. While miR122 does not directly target known fatty acid-related molecules based on sequence similarities, the results of this study may explain the molecular mechanism linking miR122 silencing to decreased fatty acid and cholesterol levels.

We previously reported that silencing miR122 leads to decreased SOCS3 expression levels and increased SOCS3 promoter methylation in a Dnmt1-independent manner [10]. Such correlations in human clinical tissues were confirmed in most cases in this study. However, some cases did not show such a correlation, perhaps because while SOCS3 expression is mainly regulated by methylation of its promoter [16,17], such modifications are probably not mediated solely by miR122. Nonetheless, the decrease in SOCS3 expression that frequently accompanies decreased miR122 expression in chronic liver pathological states suggests that the SOCS3 expression in hepatocytes is largely regulated by miR122 expression or function.

The expression of SREBP1 is negatively regulated by activated STAT3, which inhibits SREBP1 promoter activities [9]. Decreased SREBP1 expression caused by increased STAT3 activity, which was itself due to decreased SOCS3 expression, was observed in miR122-silenced Huh7 cells and in liver tissues with decreased miR122 expression. Because miR122 expression levels tend to decrease as the pathological status of the liver progresses from chronic hepatitis to liver cirrhosis [11,15], observing a decreased synthesis of fatty acid and cholesterol in progressed chronic liver diseases such as liver cirrhosis may be reasonable.

One complex liver pathological situation from this point of view is obese subjects with fatty liver and insulin resistance. In these subjects, persistently elevated cytokine levels may have downregulated STAT3-mediated signaling by increasing SOCS3 protein levels in the liver [18]. Increased SOCS3 protein levels may in turn increase fatty acid synthesis by upregulating SREBP1 expression, presumably through suppression of STAT3 activation [18]. Overproduction of fatty acids and lipotoxicity result in further insulin resistance [19]. However, as these pathological conditions persist, liver cirrhosis gradually becomes apparent and fatty acid synthesis decreases. At this stage, miR122 expression in the liver becomes low [11]. Thus, in these cases, the effects of decreased miR122 expression may become apparent for the first time at the later stages of disease progression, which may be one of the reasons why not all cases showed an exact correlation between miR122 expression and SREBP levels in clinical samples.

Recently, miravirsen, an anti-miR122 oligonucleotide, was successfully applied as a novel therapeutic against HCV [7]. Although the main purpose of applying antisense miR122 *in vivo* is at present to inhibit HCV replication, decreased fatty acid and cholesterol levels were also reported [7]. In several *in vivo* experiments, antisense miR122 reduced serum lipid levels [3–5]. In addition, mice with a miR122 gene deletion in the liver showed reduced fatty acid and cholesterol levels [2,20], despite SREBP1 not being a direct target of miR122. The molecular pathway reported here may explain the reduced lipid levels observed in miR122 inhibition or gene deletion. Moreover, from these results, inhibiting miR122 may be a promising approach to controlling serum lipid levels, although the long-term inhibition of miR122 must be confirmed to be safe with no unfavorable consequences because miRNAs have pleiotropic effects [21,22].

Author contributions

C.S. and M.O. planned the research and wrote the paper. C.S., T.K., M.O., M.O., T.Y., and A.Y. performed the majority of the experiments. H.Y. supported several experiments. K.K. supervised the entire project.

Acknowledgments

This work was supported by Grants-in-Aid from the Ministry of Education, Culture, Sports, Science and Technology, Japan (#25293076 and #24390183) (to M.O. and K.K.), by Health Sciences Research Grants of The Ministry of Health, Labour and Welfare of Japan (to K.K.), and a Grant from the Japanese Society of Gastroenterology (to M.O.).

Appendix A. Supplementary data

Supplementary data associated with this article can be found, in the online version, at http://dx.doi.org/10.1016/j.bbrc.2013.07.064.

References

[1] P. Landgraf, M. Rusu, R. Sheridan, A. Sewer, N. Iovino, A. Aravin, S. Pfeffer, A. Rice, A. Kamphorst, M. Landthaler, C. Lin, N. Socci, L. Hermida, V. Fulci, S. Chiaretti, R. Foà, J. Schliwka, U. Fuchs, A. Novosel, R. Müller, B. Schermer, U. Bissels, J. Inman, Q. Phan, M. Chien, D. Weir, R. Choksi, G. De Vita, D. Frezzetti, H. Trompeter, V. Hornung, G. Teng, G. Hartmann, M. Palkovits, R. Di Lauro, P. Wernet, G. Macino, C. Rogler, J. Nagle, J. Ju, F. Papavasiliou, T. Benzing, P. Lichter, W. Tam, M. Brownstein, A. Bosio, A. Borkhardt, J. Russo, C. Sander, M. Zavolan, T. Tuschl, A mammalian microRNA expression atlas based on small RNA library sequencing, Cell 129 (2007) 1401–1414.

[2] S.H. Hsu, B. Wang, J. Kota, J. Yu, S. Costinean, H. Kutay, L. Yu, S. Bai, K. La Perle, R.R. Chivukula, H. Mao, M. Wei, K.R. Clark, J.R. Mendell, M.A. Caligiuri, S.T. Jacob, J.T. Mendell, K. Ghoshal, Essential metabolic, anti-inflammatory, and anti-tumorigenic functions of miR-122 in liver, J. Clin. Invest. 122 (2012) 2871–2883.

[3] R.E. Lanford, E.S. Hildebrandt-Eriksen, A. Petri, R. Persson, M. Lindow, M.E. Munk, S. Kauppinen, H. Ørum, Therapeutic silencing of microRNA-122 in primates with chronic hepatitis C virus infection, Science 327 (2010) 198–201.

[4] J. Elmén, M. Lindow, S. Schütz, M. Lawrence, A. Petri, S. Obad, M. Lindholm, M. Hedtjärn, H.F. Hansen, U. Berger, S. Gullans, P. Kearney, P. Sarnow, E.M. Straarup, S. Kauppinen, LNA-mediated microRNA silencing in non-human primates, Nature 452 (2008) 896–899.

[5] C. Esau, S. Davis, S.F. Murray, X.X. Yu, S.K. Pandey, M. Pear, L. Watts, S.L. Booten, M. Graham, R. McKay, A. Subramaniam, S. Propp, B.A. Lollo, S. Freier, C.F. Bennett, S. Bhanot, B.P. Monia, MiR-122 regulation of lipid metabolism revealed by *in vivo* antisense targeting, Cell Metab. 3 (2006) 87–98.

[6] J. Krützfeldt, N. Rajewsky, R. Braich, K. Rajeev, T. Tuschl, M. Manoharan, M. Stoffel, Silencing of microRNAs *in vivo* with 'antagomirs', Nature 438 (2005) 685–689.

[7] H.L. Janssen, H.W. Reesink, E.J. Lawitz, S. Zeuzem, M. Rodriguez-Torres, K. Patel, A.J. van der Meer, A.K. Patick, A. Chen, Y. Zhou, R. Persson, B.D. King, S. Kauppinen, A.A. Levin, M.R. Hodges, Treatment of HCV Infection by targeting MicroRNA, N. Engl. J. Med. 368 (2013) 1685–1694.

[8] J.D. Horton, Sterol regulatory element-binding proteins: transcriptional activators of lipid synthesis, Biochem. Soc. Trans. 30 (2002) 1091–1095.

[9] K. Ueki, T. Kondo, Y.H. Tseng, C.R. Kahn, Central role of suppressors of cytokine signaling proteins in hepatic steatosis, insulin resistance, and the metabolic syndrome in the mouse, Proc Natl Acad Sci U S A 101 (2004) 10422–10427.

[10] T. Yoshikawa, A. Takata, M. Otsuka, T. Kishikawa, K. Kojima, H. Yoshida, K. Koike, Silencing of microRNA-122 enhances interferon-[agr] signaling in the liver through regulating SOCS3 promoter methylation, Sci. Rep. 2 (2012).

[11] R.T. Marquez, S. Bandyopadhyay, E.B. Wendlandt, K. Keck, B.A. Hoffer, M.S. Icardi, R.N. Christensen, W.N. Schmidt, A.P. McCaffrey, Correlation between microRNA expression levels and clinical parameters associated with chronic hepatitis C viral infection in humans, Lab Invest. 90 (2010) 1727–1736.

[12] K. Kojima, A. Takata, C. Vadnais, M. Otsuka, T. Yoshikawa, M. Akanuma, Y. Kondo, Y.J. Kang, T. Kishikawa, N. Kato, Z. Xie, W.J. Zhang, H. Yoshida, M. Omata, A. Nepveu, K. Koike, MicroRNA122 is a key regulator of α-fetoprotein expression and influences the aggressiveness of hepatocellular carcinoma, Nat. Commun. 2 (2011) 338.

[13] S. Bai, M. Nasser, B. Wang, S. Hsu, J. Datta, H. Kutay, A. Yadav, G. Nuovo, P. Kumar, K. Ghoshal, MicroRNA-122 inhibits tumorigenic properties of hepatocellular carcinoma cells and sensitizes these cells to sorafenib, J. Biol. Chem. 284 (2009) 32015–32027.

[14] A. Yoshimura, The CIS family: negative regulators of JAK-STAT signaling, Cytokine Growth Factor Rev. 9 (1998) 197–204.

[15] K. Morita, A. Taketomi, K. Shirabe, K. Umeda, H. Kayashima, M. Ninomiya, H. Uchiyama, Y. Soejima, Y. Maehara, Clinical significance and potential of hepatic microRNA-122 expression in hepatitis C, Liver Int. 31 (2011) 474–484.

[16] B. He, L. You, K. Uematsu, K. Zang, Z. Xu, A.Y. Lee, J.F. Costello, F. McCormick, D.M. Jablons, SOCS-3 is frequently silenced by hypermethylation and suppresses cell growth in human lung cancer, Proc. Natl. Acad. Sci. USA 100 (2003) 14133–14138.

[17] Y. Niwa, H. Kanda, Y. Shikauchi, A. Saiura, K. Matsubara, T. Kitagawa, J. Yamamoto, T. Kubo, H. Yoshikawa, Methylation silencing of SOCS-3 promotes

cell growth and migration by enhancing JAK/STAT and FAK signalings in human hepatocellular carcinoma, Oncogene 24 (2005) 6406–6417.
[18] H. Tilg, The role of cytokines in non-alcoholic fatty liver disease, Dig. Dis. 28 (2010) 179–185.
[19] V.T. Samuel, K.F. Petersen, G.I. Shulman, Lipid-induced insulin resistance: unravelling the mechanism, Lancet 375 (2010) 2267–2277.
[20] W.C. Tsai, S.D. Hsu, C.S. Hsu, T.C. Lai, S.J. Chen, R. Shen, Y. Huang, H.C. Chen, C.H. Lee, T.F. Tsai, M.T. Hsu, J.C. Wu, H.D. Huang, M.S. Shiao, M. Hsiao, A.P. Tsou, MicroRNA-122 plays a critical role in liver homeostasis and hepatocarcinogenesis, J. Clin. Invest. 122 (2012) 2884–2897.
[21] G. Szabo, P. Sarnow, S. Bala, MicroRNA silencing and the development of novel therapies for liver disease, J. Hepatol. 57 (2012) 462–466.
[22] S.P. Nana-Sinkam, C.M. Croce, Clinical applications for microRNAs in cancer, Clin. Pharmacol. Ther. 93 (2013) 98–104.
[23] A. Takata, M. Otsuka, T. Yoshikawa, T. Kishikawa, Y. Hikiba, S. Obi, T. Goto, Y.J. Kang, S. Maeda, H. Yoshida, M. Omata, H. Asahara, K. Koike, MicroRNA-140 acts as a liver tumor suppressor by controlling NF-κB activity by directly targeting DNA methyltransferase 1 (Dnmt1) expression, Hepatology 57 (2013) 162–170.

Virology 450-451 (2014) 13–23

Contents lists available at ScienceDirect

Virology

journal homepage: www.elsevier.com/locate/yviro

In vitro selection of the 3′-untranslated regions of the human liver mRNA that bind to the HCV nonstructural protein 5B

Kazuhito Yuhashi [a], Shin Ohnishi [a], Tatsuhiko Kodama [b], Kazuhiko Koike [a], Hiroshi Kanamori [a,*]

[a] *Department of Gastroenterology, Graduate School of Medicine, The University of Tokyo, 7-3-1 Hongo, Bunkyo-ku, Tokyo 113-8655, Japan*
[b] *Laboratory for Systems Biology and Medicine, Research Center for Advanced Science and Technology, The University of Tokyo, 4-6-1 Komaba, Meguro-ku, Tokyo 153-8904, Japan*

ARTICLE INFO

Available online 18 December 2013

Keywords:
HCV
NS5B
LGALS1 (GAL-1)
mRNA 3′-UTR
RPS4X

ABSTRACT

Hepatitis C virus (HCV) nonstructural protein 5B (NS5B) has RNA-dependent RNA polymerase (RdRp) activity. Because NS5B recognizes various RNA motifs besides the HCV genome, NS5B has the potential of interacting with host RNA molecules. In this study, an RNA pool enriched with the 3′-UTR sequences was generated and mRNA molecules with high affinity binding to NS5B were selected by iterative selection. Among the high binding mRNA 3′-UTR segments, we analyzed the housekeeping ribosomal protein S4, X-linked [RPS4X] mRNA 3′-UTR and the 3′-UTR of galectin-1 (GAL-1) mRNA, which is known to be one of the genes upregulated in HCV-infected liver cells and to have a wide spectrum of biological properties. By means of IP-RT-PCR, it was demonstrated that both of the mRNA molecules bind to NS5B in the cytoplasm. Interestingly, GAL-1 and RPS4X mRNA can serve as templates for NS5B RdRp, suggesting these RNA molecules are regulated *in vivo* by NS5B.

Introduction

Hepatitis C virus (HCV) is a member of the *Flaviviridae* family and contains a positive-sense, single-stranded RNA genome of approximately 9.6 kb (Choo et al., 1989; Kato et al., 1990; Takamizawa et al., 1991), which encodes 4 structural and 6 nonstructural viral proteins (Eckart et al., 1993; Grakoui et al., 1993; Lin et al., 1994; De Francesco 1999). The nonstructural protein 5B (NS5B), which has RNA-dependent RNA polymerase (RdRp) activity (Behrens et al., 1996), has been shown to play a pivotal role in the replication process of the virus. Purified NS5B transcribes the full-length HCV RNA *in vitro* via a copy-back mechanism (Lohmann et al., 1997) and/or *de novo* replication (Luo et al., 2000). Although the crystal structure of NS5B has been determined (Lesburg et al., 1999; Bressanelli et al., 1999; Ago et al., 1999) and the host cellular factors required for HCV replication have been identified (Poenisch and Bartenschlager, 2010), the mechanism of HCV replication is still not completely clear.

The 3′-non-coding region of HCV is composed of variable sequences of approximately 40 nucleotides, a poly(U/UC) tract, and a highly conserved 98-nucleotide 3′-terminal segment termed 3′X (Kolykhalov et al., 1996; Tanaka et al., 1995; Yamada et al., 1996). Earlier studies showed that NS5B binds to both the 3′X RNA and the poly(U/UC) tract (Cheng et al., 1999; Oh et al., 2000). More recent studies have indicated that NS5B binds also to cognate coding sequences (Kim et al., 2002; Lee et al., 2004). Our previous study revealed that one of the stem-loop structures in the NS5B coding region, 5BSL3.2, which is indispensable for viral replication, binds tightly to NS5B (Kanamori et al., 2009). The complimentary strand of 5BSL3.2 RNA, which forms a similar secondary structure to the positive strand, was also shown to bind to NS5B, suggesting the mechanistic importance of the RNA-protein interaction for synthesis of the plus-strand (Kanamori et al., 2010). The 5BSL3.2 RNA sequence interacts not only with the NS5B protein but also with its *cis*-acting elements on the RNA genome, resulting in the formation of a replication initiation complex in association with cellular proteins. The 5BSL3.2 stem-loop structure and the distant stem-loop structure (SL2) in the 3′X region have been shown to form a pseudoknot (Friebe et al., 2005). More recent study has shown that 5BSL3.2 interacts with domain IIId of the internal ribosome entry site located in the 5′-UTR (Romero-Lopez and Berzal-Herranz, 2009).

Beside its own genomic RNA, NS5B has been shown to be able to utilize diverse RNA molecules such as rat dimerization cofactor of hepatocyte nuclear factor-1α (Behrens et al., 1996), various homopolymers (Lohmann et al., 1997) and certain synthetic RNA molecules (Kao et al., 2000) as its RdRp templates. On the other hand, certain template RNA sequence requirement for NS5B to synthesize the anti-strand RNA does appear to exist. Strict

* Corresponding author. Tel./fax: +81 3 5800 8901.
E-mail address: hkanamori-tky@umin.net (H. Kanamori).

0042-6822/$ - see front matter © 2013 Elsevier Inc. All rights reserved.
http://dx.doi.org/10.1016/j.virol.2013.11.036

sequence-specific RdRp activities of NS5B on RNA molecules have been demonstrated in experiments using artificial RNA stem-loop structures (Kanamori et al., 2009; Kao et al., 2000; Biroccio et al., 2002; Vo et al., 2003).

Thus, NS5B can bind to or replicate several different RNA motifs depending on the sequence and structure of the RNA. In virus-infected cells, certain viral proteins such as the SOX protein Kaposi's sarcoma-associated herpes virus and the vaccinia D10 protein regulate cellular RNA expression through direct interactions (Lee and Glaunsinger, 2009; Parrish et al., 2007). The wide spectrum of NS5B RNA recognition suggests the possible interaction of NS5B with cellular mRNA molecules and regulation of these mRNA species by NS5B in the infected cells. In fact, the HCV products appear to induce an increase or decrease in the expression levels of cellular genes associated with cellular defense mechanisms, cellular metabolism or intracellular transport (Blackham et al., 2010). Among these genes, GlcT-1 (ceramide glucosyltransferase) expression is known to be induced by NS5B (Guo et al., 2012).

The mRNA 3′-UTRs have been intensively investigated in studies of the RNA binding proteins, in part because the mRNA 3′-UTRs are more accessible to cellular factors than are the coding regions of mRNA, which usually form polyribosomes in association with ribosomes (Warner et al., 1963; McCarthy and Kollmus, 1995; Levine et al., 1993; Antic et al., 1999; Imai et al., 2001).

In the present study, we constructed an RNA library that mainly contained the 3′-UTR portions of human liver cell line mRNA, selected RNA species that were found to bind tightly to the NS5B

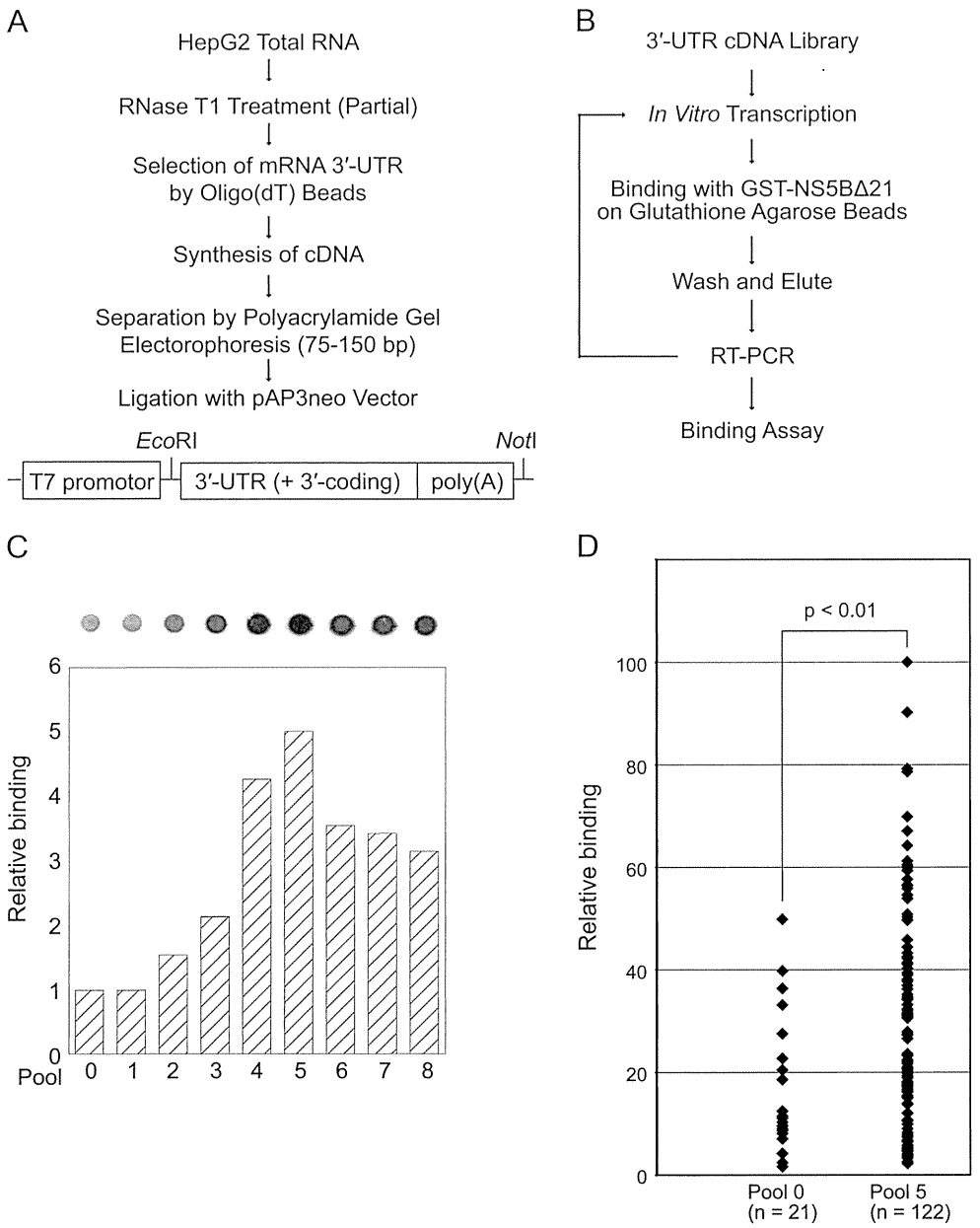

Fig. 1. Outline of the *in vitro* selection for high affinity binding hepatic mRNA 3′-UTR sequences to the HCV NS5B protein. (A) Construction of a hepatic cDNA library enriched with 3′-UTR sequences. The bottom portion indicates the construction of the template plasmids for the mRNA 3′-UTR library. (B) Scheme for *in vitro* selection of the mRNA 3′-UTRs that exhibit high-affinity binding to NS5B. (C) Relative binding to NS5B was determined by filter binding analysis and is represented by a bar graph. The dot blot analysis of the RNA pools from the different selection cycles is shown at the top. The relative binding of pool 0 was set at 1. (D) The relative binding strength of the individual clones from pool 0 (n=21) and pool 5 (n=122) was determined by filter binding dot blot analysis. The binding strength of each clone was plotted relative to that of the highest binder, RPS5 3′-end mRNA, which was set at 100. The significance of the difference in binding ability to NS5B between pools 0 and 5 RNA clones was analyzed by Welch's t-test.

protein of HCV by employing iterative selection cycles, and identified mRNA 3′-UTRs that can be templates of the NS5B polymerase.

Results

Selection of mRNA 3′-UTR sequences that bind tightly to the HCV NS5B protein

We constructed a cDNA library that mostly consisted of 3′-UTR sequences plus poly(A) tails (Fig. 1A). The 3′-UTR mRNA portion varies in length, ranging from less than 50 to over 5,000 nucleotides, with many of the mRNA 3′-UTRs around a 100-nucleotide length (Grillo et al., 2010). To construct a cDNA library enriched with the 3′-UTR sequences, we added a step in which partial digestion of the total RNA from HepG2 cells with RNase T1 was included. After the synthesis of cDNA from the partially digested liver cell poly(A) RNA, the cDNA with a length between 75 and 150 nucleotides was constructed under the T7 promoter to generate the templates for the initial RNA library for the selection. We estimated that the library contained approximately 10^5 independent clones. By sequence analysis of the library (40 clones), we found that the cDNA clones contained 3′-UTRs of 15–105 nucleotides in length (on average 56.2 nucleotides) and the poly(A) tails (on average 18 nucleotides). The initial RNA pool (pool 0) was synthesized by *in vitro* transcription using the cDNA library as a template.

By applying a selection cycle using GST-NS5B (genotype 1b, strain BK) as the target molecule (Fig. 1B), we obtained RNA clones with stronger binding to NS5B. In the selection procedure, the bound poly(A)+ RNA molecules to NS5B were recovered, amplified by RT-PCR, *in vitro* transcribed and subjected to iterative selection cycles. The binding capacities of each RNA pool was

Table 1
Genes for which the 3′-RNA sequences bind tightly to HCV NS5B.

Symbol	Accession	Gene name	Expression level[a]	Relative binding[b]	
				clone	3′-UTR
RPS5	NM_001009.3	Ribosomal protein S5	2460.5	100	68
ATP5I	NM_007100.2	ATP synthase, H+ transporting, mitochondrial F0 complex, subunit E, nuclear gene encoding mitochondrial protein	470.6	90	ND
C5	NM_001735.2	Complement component 5	189.5	79	ND
GNB2L1	NM_006098.4	Guanine nucleotide binding protein (G protein), beta polypeptide 2-like 1	2869.2	70	96
NFS1	NM_021100.3	NFS1 nitrogen fixation 1 homolog (S. cerevisiae), nuclear gene encoding mitochondrial protein	155.4	67	ND
RPS15A	NM_001019.4	Ribosomal protein S15a, transcript variant 2	4826.1	64	33
RPS4X	NM_001007.3	Ribosomal protein S4, X-linked	3404.1	61	85
RPL41	NM_001035267.1	Ribosomal protein L41, transcript variant 2	5374.1	60	93
LGALS1 (GAL-1)	NM_002305.3	Lectin, galactoside-binding, soluble, 1 (galectin-1)	80.1	59	100

[a] The relative expression level of each gene in HepG2 human hepatoblastoma cells was determined using CHIP (HG-U133A) from the Reference database for gene expression analysis: RefExA (http://157.82.78.238/refexa/main_search.jsp).

[b] The relative binding strength of each pool 5 RNA clone to GST-NS5B was determined by dot blot experiments. The binding strength of the RPS5 clone was set equal to 100. The relative binding strength of the 3′-UTR RNA sequence (47 nucleotides) of each gene to GST-NS5B was determined by the RNA gel mobility shift analysis shown in Fig. 2A. The binding strength of the GAL-1 3′-UTR was set equal to 100.

Table 2
Frequency of each selected gene in pool 0 and pool 5.

Gene	Nucleotide length[a]		Frequency		Functional category
	Coding	3′-UTR	Pool 0	Pool 5	
RPS5	30 (615)	60	1/67	1/188	Structural constituent of ribosome
ATP5I	10 (210)	61	0/67	1/188	Contributes to ATPase activity, hydrogen ion transmembrane transporter activity, transmembrane transporter activity
C5	0 (5031)	72 (401)	0/67	1/188	C5a anaphylatoxin chemotactic receptor binding, chemokine activity, endopeptidase inhibitor activity, receptor binding
GNB2L1	39 (954)	21	0/67	2/188	GTPase activity, protein kinase C binding, receptor activity, kinase activity
NFS1	0 (1374)	93 (657)	0/67	1/188	Cysteine desulfurase activity, protein binding, protein homodimerization activity, pyridoxal phosphate binding
RPS15A	51 (393)	41	0/67	5/188	structural constituent of the ribosome
RPS4X	4 (792)	64	0/67	4/188	RNA binding, rRNA binding, structural constituent of the ribosome
RPL41	0 (78)	79 (308)	1/67	3/188	Structural constituent of the ribosome
LGALS1 (GAL-1)	44 (408)	51	0/67	1/188	Galactose binding, promotes apoptosis of activated T cells, regulation of CD4+CD25+ T cells, tumor-immune escape and correlation with tumor aggressiveness
Total			2/67 (0.030)	19/188 (0.101)	

[a] Nucleotide length of coding and 3′-UTR lesions of each selected clone is indicated. In the parenthesis, the nucleotide length of the full length coding or 3′-UTR of each cDNA is indicated.